The application of diamondoid indices in the Tarim oils

Yun Li, Yongqiang Xiong, Qianyong Liang, Chenchen Fang, Yuan Chen, Xiaotao Wang, Zewen Liao, and Ping'an Peng

ABSTRACT

This study presents new data for the identification of the source and assessment of the thermal maturity of oils based on the diamondoid indices of oils from the Tazhong and Luntai uplifts in the Tarim Basin in northwest China. The oil samples were divided into three groups according to biomarker characteristics and the abundance and distribution of diamondoids. Group I oils are located along the Tazhong No. 1 fault zone, which contained abundant diamondoids and are of high thermal maturity, suggesting they are late-charged hydrocarbons that were derived from a Middle–Upper Ordovician source. Group II oils are mainly located in blocks close to the Tazhong No. 1 fault zone and are dominated by early formed hydrocarbons from Cambrian–Lower Ordovician source rocks. Group III lacustrine oils comprise relatively low concentrations of diamondoids compared with group I and group II oils. Group III oils were sourced from Jurassic or possibly Triassic units and are hosted by the low-relief Yingmaili section of the Luntai uplift. The thermal maturity of the oils in each group was evaluated using diamondoid parameters; a few group I oils exhibit intense thermal cracking. To estimate the extent of oil cracking using the concentrations of diamondoids in oils, this study proposes a practical approach that facilitates the determination of baseline 4- and 3-methyldiamantane concentrations. Application of this method indicates that the Tarim Basin marine oils contain a baseline concentration of approximately 69 ppm.

INTRODUCTION

The Tarim Basin is a large petroliferous basin in northwest China and covers an area of 560,000 km^2 (216,217 mi^2) (Figure 1A)

AUTHORS

YUN LI ~ State Key Laboratory of Organic Geochemistry, Guangzhou Institute of Geochemistry, Chinese Academy of Sciences, 511 Kehua Street, Wushan, Tianhe District, Guangzhou, Guangdong 510640, PR China; liyun@gig.ac.cn

Yun Li graduated from China University of Geosciences (Wuhan) with a B.S. degree in petroleum geology in 2006. In 2011, she completed her Ph.D. at Guangzhou Institute of Geochemistry, Chinese Academy of Sciences, where she studied oil and gas geochemistry, isotope geochemistry, and organic geochemistry. She currently works in the hydrocarbon accumulation in deep petroleum systems in China.

YONGQIANG XIONG ~ State Key Laboratory of Organic Geochemistry, Guangzhou Institute of Geochemistry, Chinese Academy of Sciences, 511 Kehua Street, Wushan, Tianhe District, Guangzhou, Guangdong 510640, PR China; xiongyq@gig.ac.cn

Yongqiang Xiong received his Ph.D. from the Guangzhou Institute of Geochemistry, Chinese Academy of Sciences, in geochemistry in 2001. His general research interest is oil and gas geochemistry. His present research is focused on the quantitative characterization of the source and maturity of highly mature hydrocarbons.

QIANYONG LIANG ~ Guangzhou Marine Geological Survey, 188 Guanghai Street, Huangpu District, Guangzhou, Guangdong 510760, PR China; 153464366@qq.com

Qianyong Liang received his Ph.D. from the Guangzhou Institute of Geochemistry, Chinese Academy of Sciences, in geochemistry in 2012. His general research interests include oil and gas geochemical prospecting and isotope geochemistry. His present research is focused on marine oil and gas prospecting and microbial geochemistry.

CHENCHEN FANG ~ PetroChina Research Institute of Petroleum Exploration and Development, 20 Xueyuan Street, Haidian District, Beijing 100083, PR China; 394515845@qq.com

Chenchen Fang received her Ph.D. from the Guangzhou Institute of Geochemistry, Chinese Academy of Sciences, in geochemistry in 2013 and finished her postdoctoral degree in PetroChina Research Institute of Petroleum Exploration and Development in 2015. Her general research interest is petroleum geochemistry. Her present research is focused on the oil and gas exploration in deep basins in China.

YUAN CHEN ~ State Key Laboratory of Organic Geochemistry, Guangzhou Institute of Geochemistry, Chinese Academy of Sciences, 511 Kehua Street, Wushan, Tianhe District, Guangzhou, Guangdong 510640, PR China; 196957780@qq.com

Yuan Chen graduated from China University of Geosciences (Wuhan) with a B.S. degree in geochemistry in 2009 and received her Ph.D. from the Guangzhou Institute of Geochemistry, Chinese Academy of Sciences, in geochemistry in 2015. Her general research interest is oil and gas geochemistry. Currently, she is an English editor in a consultant company.

XIAOTAO WANG ~ State Key Laboratory of Organic Geochemistry, Guangzhou Institute of Geochemistry, Chinese Academy of Sciences, 511 Kehua Street, Wushan, Tianhe District, Guangzhou, Guangdong 510640, PR China; 232082827@qq.com

Xiaotao Wang graduated from Sun Yat-sen University with a B.S. degree in geology in 2012 and received his M.S. degree from the Guangzhou Institute of Geochemistry, Chinese Academy of Sciences, in geochemistry in 2015. His general research interest is oil and gas geochemistry.

ZEWEN LIAO ~ State Key Laboratory of Organic Geochemistry, Guangzhou Institute of Geochemistry, Chinese Academy of Sciences, 511 Kehua Street, Wushan, Tianhe District, Guangzhou, Guangdong 510640, PR China; liaozw@gig.ac.cn

Zewen Liao received his Ph.D. from the Guangzhou Institute of Geochemistry, Chinese Academy of Sciences, in geochemistry in 2001. His general research interests include petroleum geochemistry and the quantitative evaluation of the mixed oil reservoirs. Currently, he is working in the

(Hanson et al., 2000). It is a Paleozoic cratonic basin that has been overprinted by the formation of Mesozoic–Cenozoic foreland depressions. The Tabei and Tazhong uplifts within the basin contain multiple hydrocarbon reservoirs that are complicated by multiple potential source rock suites and multiple phases of hydrocarbon charging, as well as secondary alteration (e.g., thermal cracking, biodegradation, mixing, and gas washing) of hydrocarbon accumulations (Hanson et al., 2000; Xiao et al., 2000; Zhang et al., 2000, 2005, 2011; Tian et al., 2008; Jia et al., 2010, 2013). Consequently, oil–oil and oil–source rock correlations are difficult to establish (Huang et al., 1999; Zhang et al., 2000, 2011).

The oils within the Tarim Basin display a wide range of API gravity and wax content (Hanson et al., 2000; Xiao et al., 2000). Previous studies have focused on using various organic geochemical methods to investigate the origin and evolution of hydrocarbons within this basin (Hanson et al., 2000; Sun et al., 2003; Zhang and Huang, 2005; Pan and Liu, 2009; Jia et al., 2010, 2013; Li et al., 2010). At least seven genetic groups of oils have been identified in the Tarim Basin (Hanson et al., 2000); the two largest oil groups are marine oils within the Tazhong and Tabei uplifts and lacustrine oils within the Yaha and Yingmaili oilfields of the Luntai uplift. The former is thought to be derived from Middle–Upper Ordovician anoxic marls within the Manjiaer depression, whereas the latter is derived from Jurassic or possibly Triassic lacustrine source rocks within the Kuche depression (Hanson et al., 2000). Oils in the Tadong area are thought to represent another type of marine oil sourced from Cambrian–Lower Ordovician units (Zhang and Huang, 2005).

However, recent research suggests that the majority of the oils within the Tabei and Tazhong uplifts have a mixed origin (Li et al., 2010; Yu et al., 2012; Jia et al., 2013). Two possible end-member oils were defined using geochemical variations: one derived from Middle–Upper Ordovician source rocks such as the Yingmai 2 (YM2) oils and the other derived from Cambrian–Lower Ordovician source rocks, such as oils in the Tadong area (Zhang and Huang, 2005; Li et al., 2010). As indicated by Yu et al. (2012), presently, only a few oils (i.e., the Tadong 2 [TD2], Fang1, and Tazhong 62 [Silurian] [TZ62(S)] oils) within this region were derived from Cambrian–Lower Ordovician source rocks.

At present, there is no consensus on the maturity levels of marine oils in the Tarim Basin. For example, Chen et al. (1996) proposed that the equivalent vitrinite values of the oils from the Lunnan and Tazhong areas are 1.4%–1.7% vitrinite reflectance (R_o) based on diamondoid parameters. Based on the methylphenanthrene index 1 (MPI-1), methyldibenzothiophene (MDBT) ratio (MDR), and the methyldiamantane (MD) index (MDI; 4-MD/[1-MD + 3-MD + 4-MD]), Zhang et al. (2005) obtained three different equivalent vitrinite ranges of marine oils from the cratonic region of the Tarim Basin, which

are 0.66%–0.97%, 1.11%–1.64%, and 0.89%–1.74% R_o, and suggested that the difference might be caused by multiple petroleum accumulations. However, the common knowledge is that the Tarim marine oils from Middle–Upper Ordovician and Cambrian–Lower Ordovician sources are generally of high maturity (Chen et al., 1996; Li et al., 2010). The relatively high thermal maturity of these oils means that majority of biomarker maturity indices are in equilibrium and cannot be used to determine the maturity of the marine oils in the study area, especially the condensates (Chen et al., 1996; Peters et al., 2005). In comparison, the higher resistance to thermal destruction and biodegradation of diamondoids relative to most other crude oil constituents means that they are ideal for determining the thermal maturity of highly mature crude oils (Chen et al., 1996; Li et al., 2000; Zhang et al., 2005). The diamondoid isomer with methyl substitution at a bridgehead position is more stable than that at a secondary carbon position because the latter is characterized by additional skew-butane repulsion that increases the activity (Wingert, 1992). With increasing thermal stress, the abundance of stable hydrocarbons will increase relative to that of the less stable ones, as shown in previous geochemical studies. Thus, the maturity indices based on diamondoid isomerization reflect the maturity variation (Chen et al., 1996; Dahl et al., 1999; Zhang et al., 2005; Wei et al., 2007). The abundance and distribution of diamondoids has previously been used to investigate the thermal maturity of oils within the Tarim Basin (Zhang et al., 2005; Li et al., 2010; Su et al., 2016), as exemplified by Ordovician oils associated with the Tazhong No. 1 fault zone. The oils from the Tazhong No. 1 fault zone contain much higher concentrations of diamondoids than other oils in this area, and the concentrations increase from west to east (Li et al., 2010). Recently, diamondoid maturity indices have been reexamined using thermal simulations of oil cracking and quantitative determination of diamondoids by gas chromatography–triple quadrupole mass spectrometry (GC–MS–MS; Fang et al., 2012, 2013).

Several diamondoid indices have been established based on systematic simulation experiments in the laboratory (Fang et al., 2012, 2013) or studies on field samples (Wei et al., 2006); however, field applications are limited (Zhang et al., 2005; Li et al., 2010). We use diamondoid indices in combination with biomarkers in this study to investigate the origin and maturity of crude oils in the Tazhong area of the Tarim Basin, China. The objectives are to (1) evaluate the applicability of diamondoid indices in petroleum geochemistry; (2) provide new insights into the origin and evolution of oils in the Tarim Basin using the diamondoids; and (3) present a method for the estimation of the methyldiamantane baseline of marine oils in the Tarim Basin, which is essential for oil cracking measurements. Traditional biomarker methods are more effective in investigating low to moderately mature oils. However,

area of biogeochemistry associated with the source rocks of the oil reservoirs.

PING'AN PENG ~ *State Key Laboratory of Organic Geochemistry, Guangzhou Institute of Geochemistry, Chinese Academy of Sciences, 511 Kehua Street, Wushan, Tianhe District, Guangzhou, Guangdong 510640, PR China; pinganp@gig.ac.cn*

Ping'an Peng received his Ph.D. from the Guangzhou Institute of Geochemistry, Chinese Academy of Sciences, in geochemistry in 1991. His general research interests include environmental geochemistry, petroleum geochemistry, and biogeochemistry. His present research is focused on the origin and accumulation of gas and oils in deep petroleum systems.

DATASHARE 90

Figures S1–S3 and Tables S1 and S2 are available in an electronic version on the AAPG website (www.aapg.org/datashare) as Datashare 90.

Figure 1. (A) Map of the Tarim Basin showing sampling locations. Modified from Hanson et al. (2000) and used with permission of AAPG. (B) Enlarged map of the sampling locations in the Tazhong uplift. (C) Schematic structural cross section AA' across the central part of the Tarim Basin. Modified from Li et al. (1996) and used with permission of AAPG. Circled numbers 1–6 refer to six unconformities recognized from the Sinian to the Cenozoic. (1) Tarim orogeny occurred in the bottom of the Sinian. (2) Caledonian orogeny occurred in the bottom of the Silurian. (3) Early Hercynian orogeny occurred in the bottom of the Carboniferous. (4) Late Hercynian orogeny occurred between the Upper Permian and the Lower Permian. (5) Indo-China orogeny occurred in the bottom of the Jurassic. (6) Late Yanshanian orogeny occurred in the bottom of the Tertiary. AnZ = Presinian; $\in$ = Cambrian; C = Carboniferous; Cz = Cenozoic; D = Devonian; J = Jurassic; K = Cretaceous; Mz = Mesozoic; O = Ordovician; P_1 = Lower Permian; P_2 = Upper Permian; Pt = Proterozoic; Pz = Paleozoic; S = Silurian; T = Triassic; TD = Tadong; TZ = Tazhong; YM = Yingmai; Z_2 = Upper Sinian; ZG = Zhonggu.
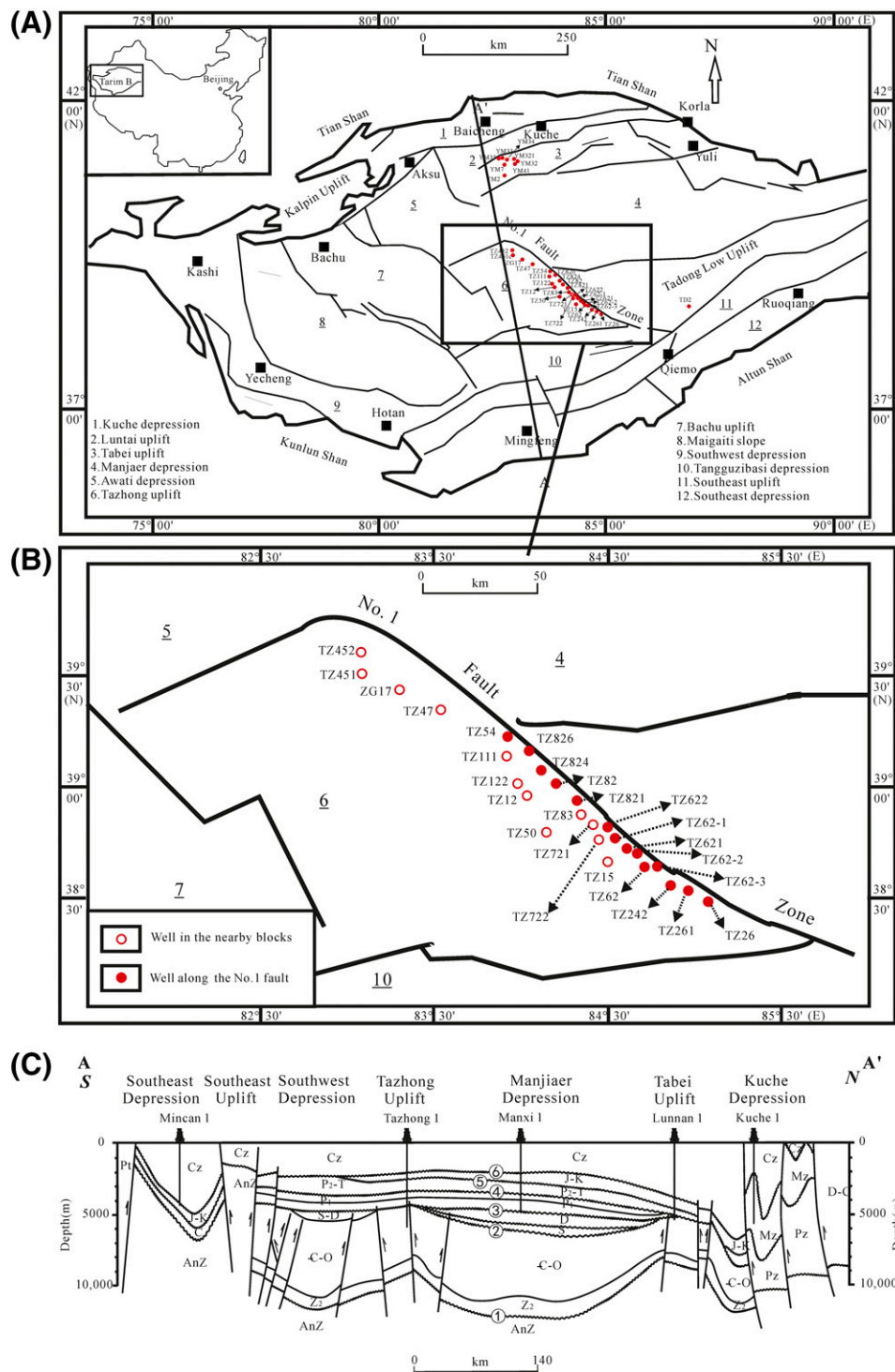
most of these methods are not feasible for highly mature oils. Diamondoid indices are considered to be a powerful tool to study highly mature oils. The combination of traditional biomarkers and diamondoid research might provide a more comprehensive understanding of mixed oils that occur within the Tazhong uplift.

GEOLOGICAL BACKGROUND

The Tarim Basin is a Paleozoic cratonic basin, which was divided into several uplifts and depressions by crustal tectonism (Figure 1A, C). Each tectonic entity has different structural, stratigraphic, and

petrological characteristics. The Tazhong and Tabei uplifts are the major hydrocarbon-rich areas in the region; most oil fields were discovered in these two areas. However, the origin of the oils in the Tazhong uplift is controversial. The Tazhong No. 1 fault is an important factor in the oil migration and accumulation of the Tazhong area (Li et al., 2010; Pang et al., 2013). Therefore, we mainly focused on the oils located along the Tazhong No. 1 fault and in nearby blocks; the oils collected from the Luntai uplift were used for comparison.

The Tazhong uplift is one of the most important regions of petroleum accumulation in the Tarim Basin, with an exploration area of approximately 22,000 km^2 (8494 mi^2) (Pang et al., 2013). It is adjacent to the southern part of the Manjiaer depression, northern part of the Tangguziba depression, eastern part of the Bachu uplift, and western part of the Tadong low uplift (Figure 1A). Based on drilling data, nearly all sedimentary strata from Sinian to Quaternary are preserved in this area (Figure 2) (Li et al., 2010). The Cambrian section is composed of platform carbonates and evaporites. The Upper Ordovician Sangtamu Formation is mainly composed of siliciclastic rocks, whereas the other Ordovician formations mainly comprise carbonate rocks. The sediments deposited during the Silurian and Devonian are sandstones and red mudstones, whereas marine clastic rocks accumulated during the Carboniferous. A sedimentary hiatus occurred during the late Permian; the renewed subsidence led to the accumulation of Mesozoic–Cenozoic terrestrial sandstones and mudstones.
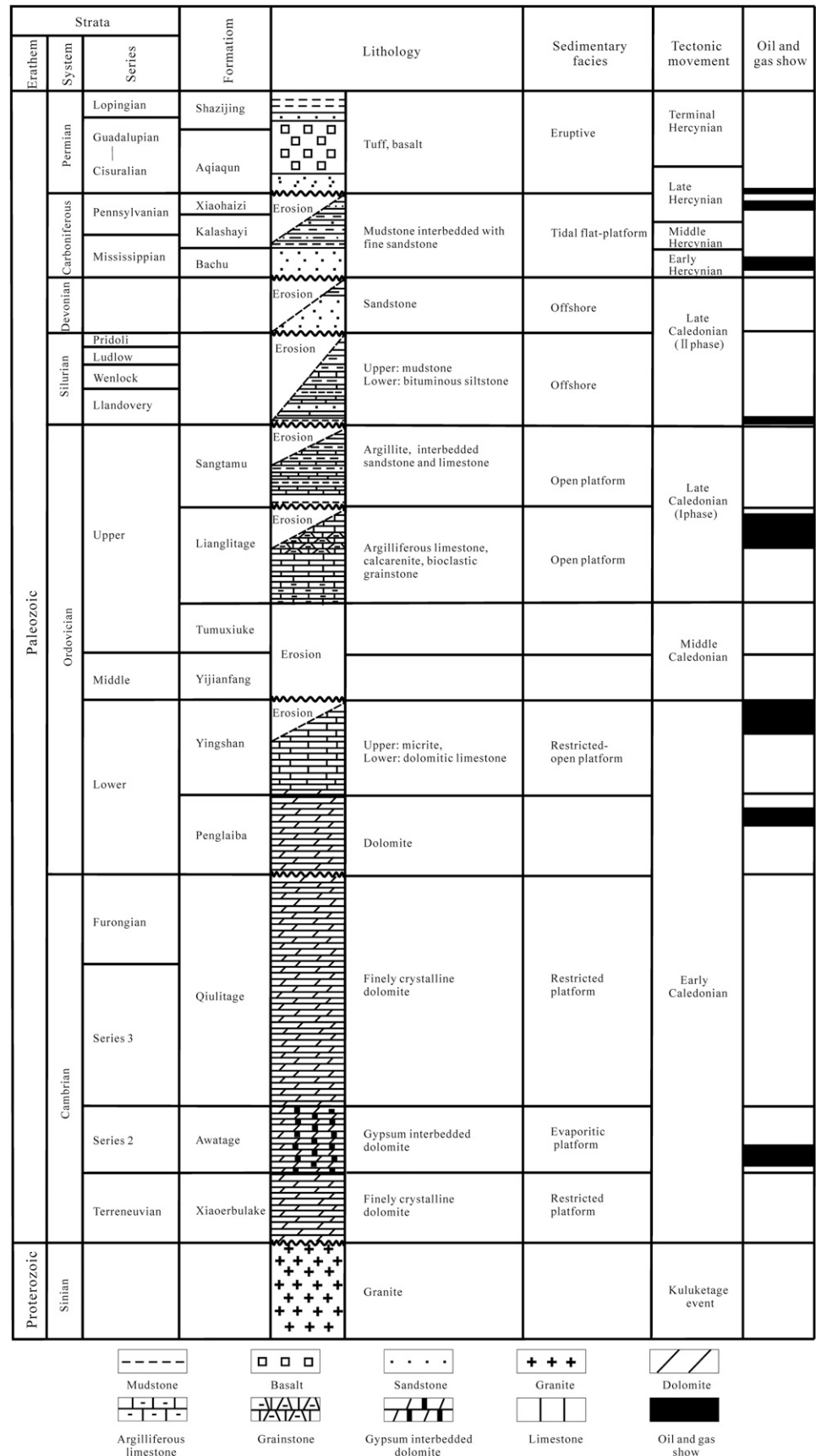
The marine oils discovered in the Tazhong uplift are considered to primarily originate from Cambrian–Lower Ordovician and Middle–Upper Ordovician strata; however, what stratum is the main hydrocarbon contributor is controversial (Hanson et al., 2000; Zhang et al., 2000; Zhang and Huang, 2005; Li et al., 2010). The Lower and Middle Cambrian source rocks in the Tarim Basin consist of marls, mudstones, and dolomites. The total organic carbon (TOC) values range from 1.24 to 5.52 wt. % (Hanson et al., 2000). Cambrian source rocks are highly mature to overmature; the vitrinite reflectance equivalence (VRE; derived from Liu et al., 1994) exceeds 3.0% in the Manjiaer depression. The purported source rocks distributed in the central horst belt in the Tazhong, Tabei, and part of the Bachu uplifts have a relatively lower

maturity, with VRE values in the range of 1.6%–2.0% (Wang et al., 2003). The Lower Ordovician rocks in the Tarim Basin are similar to the Cambrian strata with respect to the marine facies, mature to overmature thermal stress, and hydrocarbon generation history (Hanson et al., 2000; Zhang et al., 2000). The Middle–Upper Ordovician source rocks in the Tarim Basin are controlled by the depositional facies. Shelf edge and slope facies widely occur at the northern slope and crest of the Tazhong uplift. The lithologies mainly include muddy limestones and marls, with an average TOC of 0.43 wt. % and a maximum TOC of 6 wt. % (Zhang et al., 2000). The maturity of the source rocks ranges from 0.81% to 1.30% VRE (Liang et al., 2000). Open bay or gulf facies occur in the Kalpin area and the Awati depression. The source rocks include the Sargan and Yingan shales, with TOC concentrations ranging from 0.05 to 2.25 wt. % (Zhang et al., 2000). The R_o values suggest that most of the source rocks in the Kalpin area are in the highly mature stage (1.10%–1.30% VRE), whereas the source rocks in the Awati depression exceed 2% VRE (Liang et al., 2000).

The reservoir formations in the Tazhong uplift are mainly present in the Ordovician strata, including the Lower Ordovician Penglaiba Formation dolomite, Lower Ordovician Yingshan Formation weathered crust, and Upper Ordovician Lianglitage Formation reef (Pang et al., 2013) (Figure 2). Additionally, oil and gas have been discovered in the Cambrian, Silurian, and Carboniferous strata of the Tazhong uplift.

The Tazhong uplift experienced several tectonic events from the Caledonian to the Himalayan orogenies, which are illustrated in detail in Lu et al. (2004) and Li et al. (2010). Briefly, the tectonic setting was relatively stable in the early Paleozoic–Devonian, with a relatively complete stratigraphic development until the end of the Devonian when erosion occurred. During this phase, the middle–late Caledonian orogeny has given rise to the development of faults and fractures in the Tazhong uplift such as the No. 1 fault (Early to Late Ordovician). The denudation of the Silurian–Devonian sedimentary succession occurred as a result of late Caledonian and early Hercynian events. The Tazhong uplift was stable in the late Paleozoic–Cenozoic. The uplift fluctuated during the Indosinian–Himalayan; however, this had little effect on the Paleozoic structures since the Mesozoic. The faults

Figure 2. General stratigraphic column of the Tazhong uplift. Modified from Li et al. (2010).

Strata			Formation	Lithology	Sedimentary facies	Tectonic movement	Oil and gas show
Erathem	System	Series					
Paleozoic	Permian	Lopingian	Shazijing		Eruptive	Terminal Hercynian	
		Guadalupian		Tuff, basalt			
		Cisuralian	Aqiaqun			Late Hercynian	
	Carboniferous	Pennsylvanian	Xiaohaizi		Tidal flat-platform	Middle Hercynian	
			Kalashayi	Mudstone interbedded with fine sandstone			
		Mississippian	Bachu			Early Hercynian	
	Devonian			Sandstone	Offshore	Late Caledonian (II phase)	
	Silurian	Pridoli		Upper: mudstone Lower: bituminous siltstone	Offshore		
		Ludlow					
		Wenlock					
		Llandovery					
	Ordovician	Upper	Sangtamu	Argillite, interbedded sandstone and limestone	Open platform	Late Caledonian (I phase)	
			Lianglitage	Argilliferous limestone, calcarenite, bioclastic grainstone	Open platform		
			Tumuxiuke			Middle Caledonian	
		Middle	Yijianfang				
		Lower	Yingshan	Upper: micrite, Lower: dolomitic limestone	Restricted-open platform		
			Penglaiba	Dolomite			
	Cambrian	Furongian	Qiulitage	Finely crystalline dolomite	Restricted platform	Early Caledonian	
		Series 3					
		Series 2	Awatage	Gypsum interbedded dolomite	Evaporitic platform		
		Terreneuvian	Xiaoerbulake	Finely crystalline dolomite	Restricted platform		
Proterozoic	Sinian			Granite		Kuluketage event	

Legend:

Mudstone	Basalt	Sandstone
Argilliferous limestone	Grainstone	Gypsum interbedded dolomite
	Granite	Dolomite
Limestone	Oil and gas show	

and associated fractures that developed in the uplift as well as unconformities provided the main pathways for hydrocarbon migration in the Tazhong area.

The Luntai uplift is a subtectonic unit of the Tabei uplift (Figure S1, supplementary material available as AAPG Datashare 90 at www.aapg.org/datashare). It is a fault horst that formed because of the structural activities of the Yingmai 7 and Yangtake fault belts (Figure S1, supplementary material available as AAPG Datashare 90 at www.aapg.org/datashare) (Liang et al., 1998). Regionally, it is located between the Tabei uplift and the Kuche depression (Figure 1A). Sinian metamorphic rocks are exposed on the surface in the core positions of the Luntai uplift. Cambrian to Permian strata successively occur in the southern, northern, and western areas, whereas Triassic and Jurassic strata are only present on the northern and southern sides of the Luntai uplift (Liang et al., 1998). The nonmarine oils discovered in the Luntai area are thought to have been derived from Jurassic or Triassic lacustrine source rocks of the Kuche depression (Hanson et al., 2000).

SAMPLES AND METHODS

Samples and Preparation

The oil samples examined in this study were collected from the Tazhong and Luntai uplifts, including a total of 17 oil samples from the Tazhong No. 1 fault zone; 15 samples from nearby blocks, such as the Tazhong 452-111 and 12-15 blocks; and 9 samples from the Yingmaili area of the Luntai uplift (Figure 1A, Table 1). These oils cover a wide range of properties (e.g., API gravity and wax content), including normal, heavy, and waxy oils and condensates (Table 1).

The oil samples were deasphaltened using hexane in excess of crude oils (40 times the volume of oil). The deasphaltened samples were then separated into saturated, aromatic, and resin fractions in a silica gel column using hexane, hexane and dichloromethane with a ratio of 3:2 (volume/volume), and methanol, respectively. The saturated fractions were then concentrated and filled into a 4-ml sample vial for gas chromatography–mass spectrometric (GC–MS) analysis.

The samples for diamondoid determination were prepared using a simple solvent dilution. Approximately 50 mg of oil sample was added to a 4-ml glass vial; this vial was filled with isooctane and ultrasonically treated for 10 min to improve sample dissolution. After precipitating asphaltenes by centrifugation for 10 min, a volume of supernatant was transferred to a 2-ml sample vial used for autosampling. The supernatant was directly injected into the GC–MS–MS system without any further sample preparation after the addition of 100 µl of an internal standard solution.

Gas Chromatography–Mass Spectrometry

The GC–MS analysis of the saturated fraction was performed on a HP7890 gas chromatograph (GC) coupled to a mass-selective detector, equipped with a 30 m × 0.32 mm (inner diameter) HP-5 column with a film thickness of 0.25 µm. Helium was used as carrier gas, with a constant flow rate of 1.2 ml/min. The GC oven temperature was initially held at 80°C for 2 min, ramped to 290°C at 4°C/min, and then held at 290°C for 20 min. The mass spectrometer was operated in selected ion monitoring mode (mass-to-charge ratio [m/z] 191 for hopanes; m/z 217 for steranes).

Gas Chromatography–Triple Quadrupole Mass Spectrometry

The GC–MS–MS analysis was performed using a Thermo Fisher TSQ Quantum XLS instrument; details of the procedures used are given in Liang et al. (2012). In this approach, a 1-µl aliquot of each sample was injected into the GC system using an AS 3000 autosampler. The GC instrument was equipped with a PTV injector, and a DB-1 fused silica capillary column with a 50 m × 0.32 mm × 0.52 µm thickness film. These analyses used a PTV splitless mode with an inlet temperature of 300°C and a split flow at 15 ml/min following 1 min of splitless flow. Helium (99.999% purity) carrier gas was used during analysis in constant flow mode at a rate of 1.5 ml/min. The GC oven temperature was initially set at 50°C for 2 min, before increasing at 15°C/min to 80°C, 2.5°C/min to 250°C, and a final increase of 15°C/min to 300°C before being held for 10 min. Quantification of diamondoid compounds (Table 2) was undertaken using a selected reaction monitoring mode comparison between peak areas for unknowns and two internal

Table 1. Basic Data of the Oil Samples Used in This Study

Sample	Area	Well	Tectonic Unit	Depth (m [ft])	Reservoir	Type	Biomarker Group*	Diamondoid Group†
1	Tazhong No. 1 fault zone	TZ26	Tazhong uplift	4300–4360 (14,108–14,304)	O_3	Condensate (darker in color)	1	1
2		TZ26	Tazhong uplift	4300–4360 (14,108–14,304)	O_3	Condensate (lighter in color)	1	1
3		TZ261	Tazhong uplift	4348–4560 (14,265–14,961)	O_3	Condensate	1	1
4		TZ261	Tazhong uplift	4357–4380 (14,295–14,370)	O_3	Condensate	1	1
5		TZ242	Tazhong uplift	4065.15 (13,337.11)	S	Normal oil	1	1
6		TZ242	Tazhong uplift	4515.56–4546.56 (14,814.83–14,916.54)	O_3	Condensate	1	1
7		TZ62	Tazhong uplift	4052.88–4073.58 (13,296.85–13,364.76)	S	Normal oil	2	2
8		TZ62-1	Tazhong uplift	4892.07–4973.76 (16,050.10t–16,318.11)	O_3	Normal oil	1	1
9		TZ62-2	Tazhong uplift	4773–4825 (15,661–15,830)	O_3	Condensate	1	1
10		TZ62-3	Tazhong uplift	5072–5165 (16,640–16,946)	O_3	Condensate	1	1
11		TZ621	Tazhong uplift	4851–4885 (15,915–16,027)	O_3	Normal oil	1	1
12		TZ622	Tazhong uplift	4914–4925 (16,122–16,158)	O_3	Heavy oil	1	1
13		TZ82	Tazhong uplift	5430–5487 (17,815–18,002)	O_3	Condensate	1	1
14		TZ821	Tazhong uplift	5212.6–5250.2 (17,101.7–17,225.1)	O_3	Condensate	1	1
15		TZ824	Tazhong uplift	5745–5750 (18,848–18,865)	O_3	Condensate	1	1
16		TZ826	Tazhong uplift	5472–5668 (17,953–18,596)	O_3	Condensate	1	1
17		TZ54	Tazhong uplift	5832–5858 (19,134–19,219)	O_3	Condensate	1	1
18		TZ721	Tazhong uplift	5205–5505 (17,077–18,061)	O_1	Waxy oil	nd	2
19	Nearby blocks	TZ721	Tazhong uplift	5355–5505 (17,569–18,061)	O_1	Waxy oil	nd	2
20		TZ722	Tazhong uplift	4916.1–4980.4 (16,128.9–16,339.9)	O_3	Normal oil	nd	2
21		TZ83	Tazhong uplift	5433–5441 (17,825–17,851)	O_3	Condensate	nd	2
22		TZ452	Tazhong uplift	6377–6550 (20,922–21,490)	O_{1+2}	Condensate	2	2

(*continued*)

Table 1. Continued

Sample	Area	Well	Tectonic Unit	Depth (m [ft])	Reservoir	Type	Biomarker Group*	Diamondoid Group[†]
23		TZ451	Tazhong uplift	6050–6298 (19,849–20,663)	O_{1+2}	Condensate	1	2
24		ZG17	Tazhong uplift	6438–6448 (21,122–21,155)	O_{2+3}	Condensate	nd	2
25		TZ47	Tazhong uplift	4978–4986 (16,332–16,358)	S	Normal oil	1	2
26		TZ111	Tazhong uplift	4357–4364 (14,295–14,318)	S	Heavy oil	1	1
27		TZ12	Tazhong uplift	4374.5–4413.5 (14,352–14,480)	S	Heavy oil	1	1
28		TZ12	Tazhong uplift	4631.88–4733.92 (15,196.46–15,531.23)	O_3	Heavy oil	1	1
29		TZ122	Tazhong uplift	4349–4353 (14,268–14,281)	S	Heavy oil	1	1
30		TZ122	Tazhong uplift	4707.07–4733.92 (15,443.14–15,531.23)	O_3	Normal oil	1	1
31		TZ50	Tazhong uplift	4378–4385 (14,364–14,386)	S	Heavy oil	1	1
32		TZ15	Tazhong uplift	4300–4307 (14,108–14,131)	S	Heavy oil	1	1
33	Yingmaili	YM7	Tabei uplift	5212.69–5277.19 (17,102.00–17,313.62)	O	Normal oil	3	3
34		YM32	Tabei uplift	5408–5413 (17,743–17,759)	$\in$	Normal oil	3	3
35		YM321	Tabei uplift	5239–5244 (17,188–17,205)	K	Normal oil	3	3
36		YM321	Tabei uplift	5335.5–5351.3 (17,504.9–17,556.8)	$\in$	Normal oil	3	3
37		YM33	Tabei uplift	5502–5513 (18,051–18,087)	$\in$	Normal oil	3	3
38		YM34	Tabei uplift	5387.08 (17,674.15)	S	Normal oil	3	3
39		YM35	Tabei uplift	5579–5585 (18,304–18,323)	S	Normal oil	3	3
40		YM35	Tabei uplift	5623–5626 (18,448–18,458)	S	Normal oil	3	3
41		YM41	Tabei uplift	5287.95 (17,348.92)	–	Normal oil	3	3
42	Taibei	YM2	Tabei uplift	5942–5953 (19,495–19,531)	O_1	Normal oil	1	1
43	Tadong	TD2	Tadong sag	4561–5040 (14,964–16,535)	$\in$	Heavy oil	2	2

Abbreviations: – = not known; $\in$ = Cambrian; K = Cretaceous; nd = not determined; O = Ordovician; O_1 = Lower Ordovician; O_{1+2} = Lower–Middle Ordovician; O_{2+3} = Middle–Upper Ordovician; O_3 = Upper Ordovician; S = Silurian; TD = Tadong; TZ = Tazhong; YM = Yingmai; ZG = Zhonggu.
*Oils are grouped according to the biomarker characteristics.
[†]Oils are grouped according to the diamondoid characteristics.

Table 2. The Detected Diamondoid Compounds in This Study

Compound	Molecular Formula	Diamondoid Compound	Abbreviation
1	$C_{10}H_{16}$	Adamantane	A
2	$C_{11}H_{18}$	1-Methyladamantane	1-MA
3	$C_{12}H_{20}$	1,3-Dimethyladamantane	1,3-DMA
4	$C_{13}H_{22}$	1,3,5-Trimethyladamantane	1,3,5-TMA
5	$C_{14}H_{24}$	1,3,5,7-Tetramethyladamantane	1,3,5,7-TeMA
6	$C_{11}H_{18}$	2-Methyladamantane	2-MA
7	$C_{12}H_{20}$	1,4-Dimethyladamantane(cis)	1,4-DMA(cis)
8	$C_{12}H_{20}$	1,4-Dimethyladamantane(trans)	1,4-DMA(trans)
9	$C_{13}H_{22}$	1,3,6-Trimethyladamantane	1,3,6-TMA
10	$C_{12}H_{20}$	1,2-Dimethyladamantane	1,2-DMA
11	$C_{13}H_{22}$	1,3,4-Trimethyladamantane(cis)	1,3,4-TMA(cis)
12	$C_{13}H_{22}$	1,3,4-Trimethyladamantane(trans)	1,3,4-TMA(trans)
13	$C_{14}H_{24}$	1,2,5,7-Tetramethyladamantane	1,2,5,7-TeMA
14	$C_{12}H_{20}$	1-Ethyladamantane	1-EA
15	$C_{12}H_{20}$	2,6-+2,4-Dimethyladamantane	2,6- + 2,4-DMA
16	$C_{13}H_{22}$	1-Ethyl-3-methyladamantane	1-E-3-MA
17	$C_{13}H_{22}$	1,2,3-Trimethyladamantane	1,2,3-TMA
18	$C_{14}H_{24}$	1-Ethyl-3,5-dimethyladamantane	1-E-3,5-DMA
19	$C_{12}H_{20}$	2-Ethyladamantane	2-EA
20	$C_{14}H_{24}$	1,3,5,6-Tetramethyladamantane	1,3,5,6-TeMA
21	$C_{14}H_{24}$	1,2,3,5-Tetramethyladamantane	1,2,3,5-TeMA
22	$C_{15}H_{26}$	1-Ethyl-3,5,7-trimethyladamantane	1-E-3,5,7-TMA
I.S.-1	$C_{12}D_{26}$	n-Dodecane-d_{26}	nC_{12}-d_{26}
23	$C_{14}H_{20}$	Diamantane	D
24	$C_{15}H_{22}$	4-Methyldiamantane	4-MD
25	$C_{16}H_{24}$	4,9-Dimethyldiamantane	4,9-DMD
26	$C_{15}H_{22}$	1-Methyldiamantane	1-MD
27	$C_{16}H_{24}$	1,4-+2,4-Dimethyldiamantane	1,4- + 2,4-DMD
28	$C_{16}H_{24}$	4,8-Dimethyldiamantane	4,8-DMD
29	$C_{17}H_{26}$	1,4,9-Trimethyldiamantane	1,4,9-TMD
30	$C_{15}H_{22}$	3-Methyldiamantane	3-MD
31	$C_{16}H_{24}$	3,4-Dimethyldiamantane	3,4-DMD
32	$C_{17}H_{26}$	3,4,9-Trimethyldiamantane	3,4,9-TMD
I.S.-2	$C_{16}D_{34}$	n-Hexadecane-d_{34}	nC_{16}-d_{34}

Abbreviation: I.S. = internal standard.

standards, namely, n-dodecane-d_{26} for adamantanes and n-hexadecane-d_{34} for diamantanes.

RESULTS AND DISCUSSION

Source Identification

Previous studies provided two end-members based on the composition and distribution of alkanes, aromatic hydrocarbons, and biomarkers and the isotope characteristics of individual n-alkanes. Oils derived from the TD2 (sample 43) and TZ62 (sample 7) wells were suggested to be the end-member compositions for typical Cambrian–Lower Ordovician sourced marine oils within the Tarim Basin, whereas the YM2 oil (sample 42) is a representative example of an end-member oil derived from Middle–Upper Ordovician source rocks (Xiao et al., 2005; Tang and Wang, 2007; Li et al., 2010).
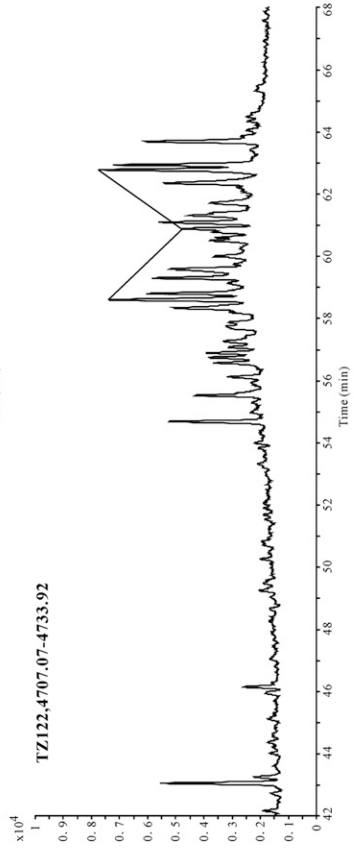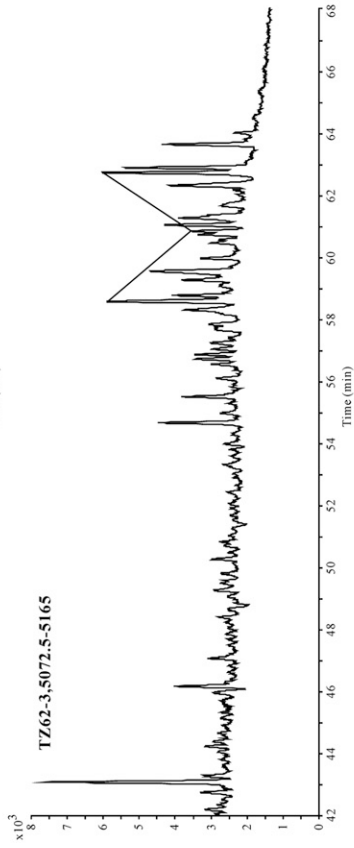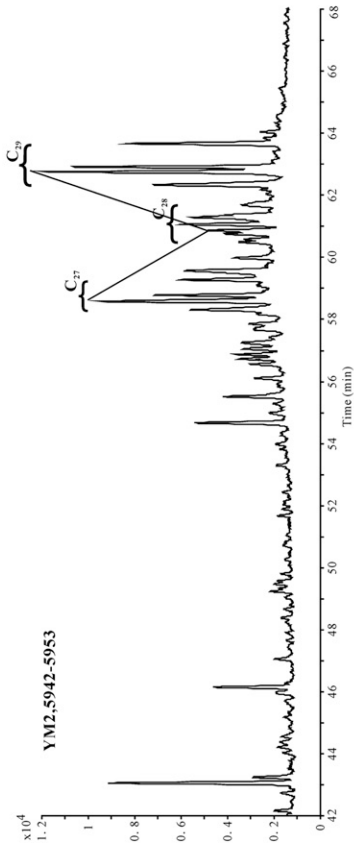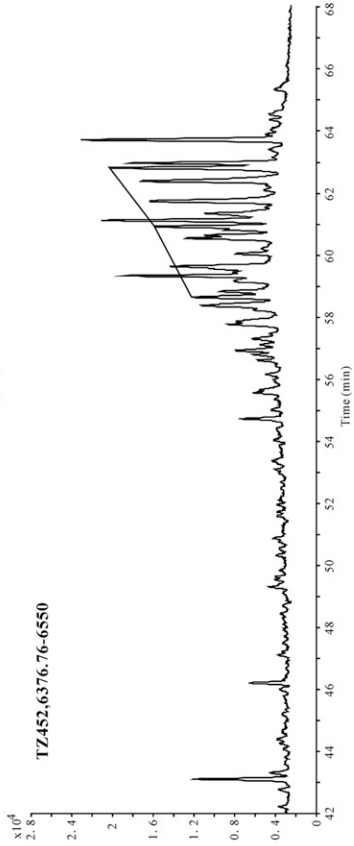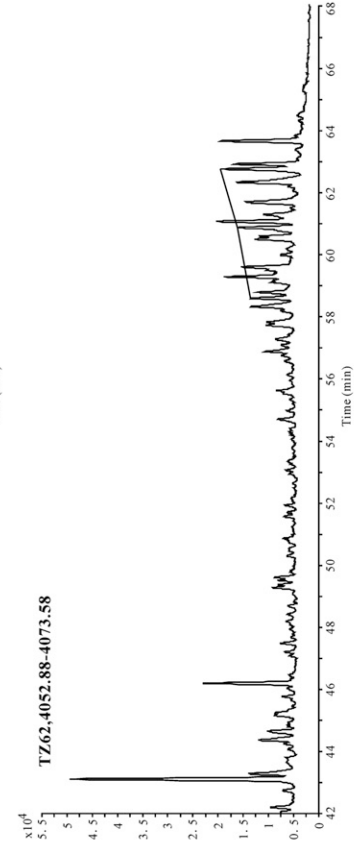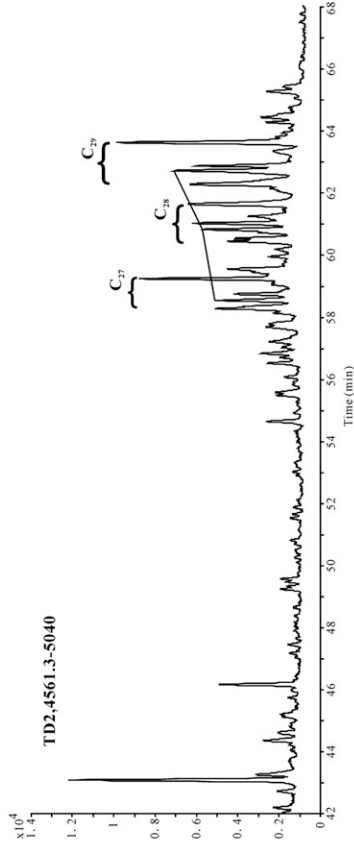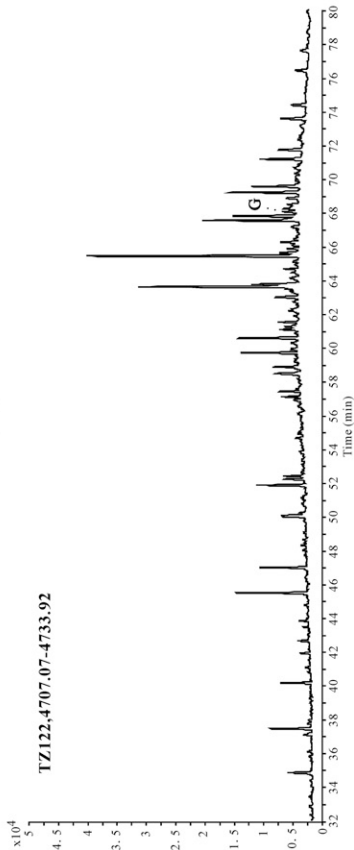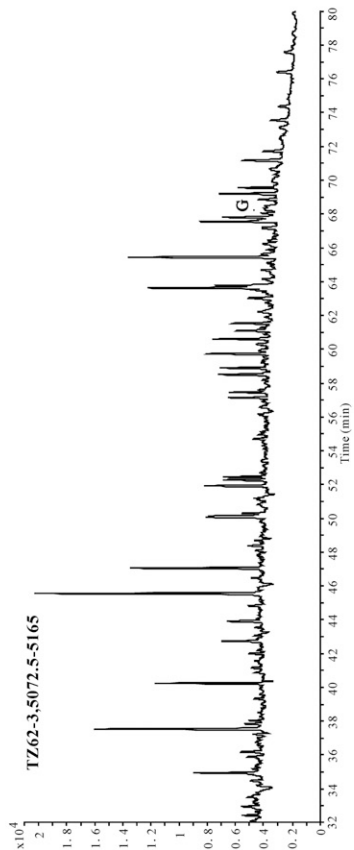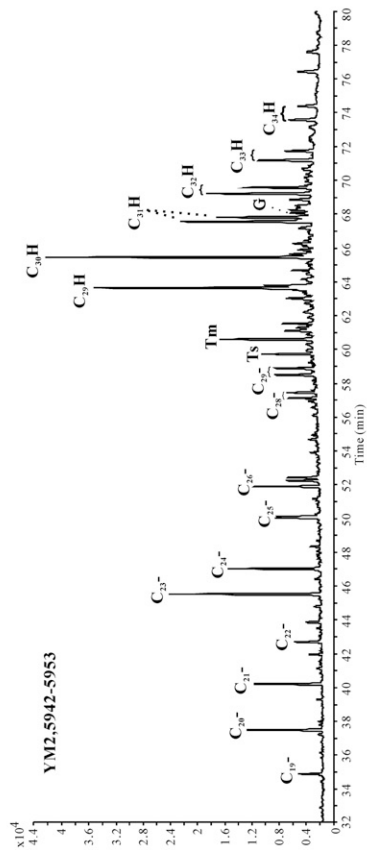
Figure 3. Mass-to-charge ratio 217 mass fragmentograms of saturated hydrocarbon fractions from selected oils, showing representative sterane distributions. TD = Tadong; TZ = Tazhong; YM = Yingmai.
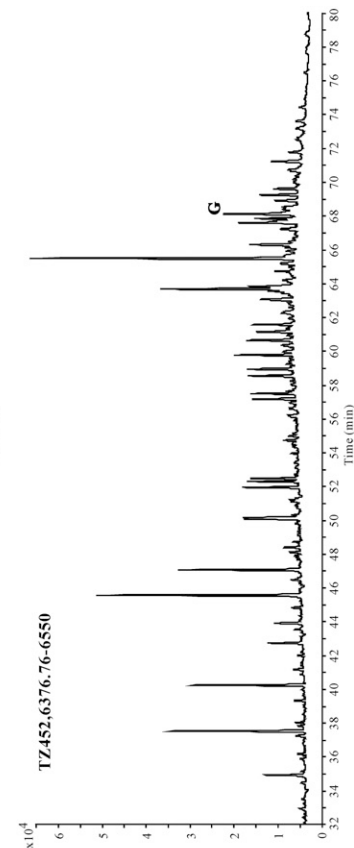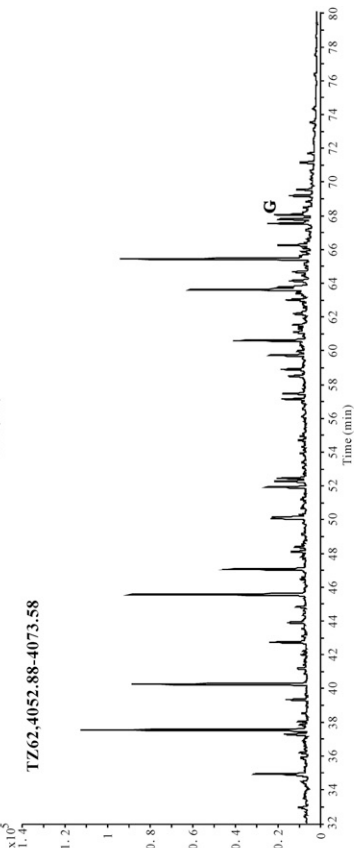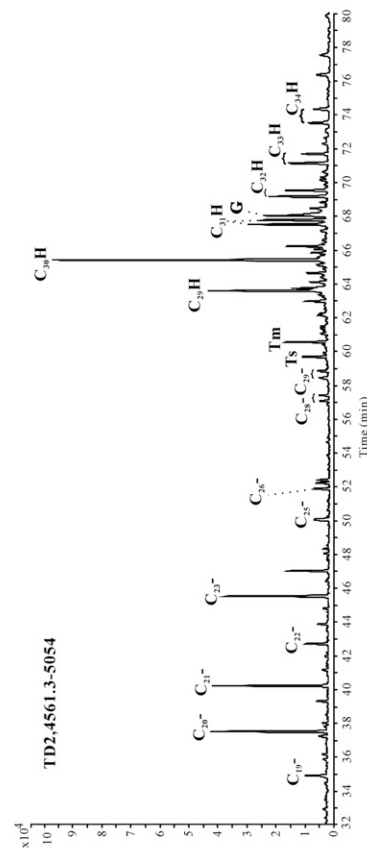
LI ET AL. **277**

Figure 4. Mass-to-charge ratio 191 mass fragmentograms of saturated hydrocarbon fractions from selected oils, showing representative tricyclic terpane and hopane distributions. C_i = C_i tricyclic terpane; C_iH = C_i hopane; G = gammacerane; TD = Tadong; Tm = 18α(H)-22,29,30-Trisnorhopane; TZ = Tazhong; YM = Yingmai. Ts = 17α(H)-22,29,30-Trisnorhopane.

Table 3. Values of Some Relevant Parameters Used in This Study

Sample	Well	Pr/Ph	Ts/(Ts + Tm)	T/(T + H)	T/P	20S	ββ	MPI-1	MDR	MDI	R_c1-1 (%)	R_c1-2 (%)	R_c2 (%)	R_c3 (%)
1	TZ26	0.82	0.48	0.22	0.34	0.51	0.50	0.65	5.60	0.49	0.79	1.91	1.36	1.63
2	TZ26	0.85	0.48	0.28	0.48	0.50	0.51	0.66	5.38	0.49	0.79	1.91	1.35	1.64
3	TZ261	0.78	0.47	0.37	0.73	0.52	0.52	0.66	4.21	0.65	0.80	1.90	1.28	2.03
4	TZ261	0.73	0.56	0.62	2.65	nd	nd	0.66	4.43	0.67	0.79	1.91	1.29	2.06
5	TZ242	0.98	0.48	0.57	1.48	0.54	0.52	0.70	4.11	0.45	0.82	1.88	1.27	1.52
6	TZ242	0.76	0.49	0.48	0.99	0.52	0.54	0.66	5.03	0.43	0.80	1.90	1.33	1.49
7	TZ62	0.89	0.36	0.49	1.39	0.50	0.43	1.28	3.03	0.37	1.17	1.53	1.19	1.35
8	TZ62-1	0.68	0.52	0.52	1.04	0.53	0.55	0.68	4.61	0.42	0.81	1.89	1.30	1.46
9	TZ62-2	0.76	0.53	0.72	2.67	0.58	0.55	0.70	5.19	0.42	0.82	1.88	1.34	1.46
10	TZ62-3	0.74	0.52	0.60	1.29	0.53	0.54	0.61	4.16	0.42	0.76	1.94	1.28	1.47
11	TZ621	0.70	0.51	0.54	1.16	0.53	0.54	0.69	4.71	0.41	0.82	1.88	1.31	1.43
12	TZ622	0.73	0.54	0.57	1.25	0.54	0.54	0.64	4.47	0.42	0.79	1.91	1.30	1.46
13	TZ82	0.77	0.53	0.43	1.00	0.52	0.52	0.76	8.24	0.42	0.86	1.84	1.46	1.46
14	TZ821	0.71	1.00	0.86	7.61	0.58	0.61	0.66	5.23	0.44	0.80	1.90	1.34	1.52
15	TZ824	0.69	0.49	0.21	0.49	0.48	0.40	0.74	16.47	0.39	0.84	1.86	1.64	1.38
16	TZ826	0.75	0.51	0.36	0.88	0.46	0.42	0.76	7.26	0.48	0.85	1.85	1.42	1.61
17	TZ54	0.74	0.54	0.36	0.93	0.49	0.45	0.67	11.32	0.41	0.80	1.90	1.54	1.43
18	TZ721	0.76	–	–	1.15	–	–	0.67	3.53	0.46	0.80	1.90	1.23	1.56
19	TZ721	0.76	–	–	8.25	–	–	0.57	3.47	0.46	0.74	1.96	1.23	1.55
20	TZ722	–	–	–	–	–	–	–	–	0.42	–	nd	nd	1.47
21	TZ83	0.78	–	–	–	–	–	0.77	8.35	0.42	0.86	1.84	1.46	1.46
22	TZ452	0.81	0.57	0.43	1.11	0.48	0.40	0.45	4.42	0.42	0.67	2.03	1.29	1.46
23	TZ451	0.75	0.83	0.79	2.82	0.58	0.56	0.71	6.22	0.40	0.83	1.87	1.38	1.42
24	ZG17	–	–	–	–	–	–	–	–	0.44	–	nd	nd	1.51
25	TZ47	0.76	0.42	0.41	0.69	0.50	0.53	0.87	6.49	0.40	0.92	1.78	1.40	1.41
26	TZ111	0.72	0.36	0.51	0.97	0.49	0.52	0.63	3.69	0.43	0.78	1.92	1.25	1.50
27	TZ12	0.85	0.41	0.26	0.40	0.48	0.47	0.91	3.46	0.40	0.94	1.76	1.23	1.42
28	TZ12	0.78	0.47	0.59	1.53	0.51	0.53	0.68	2.86	0.42	0.81	1.89	1.18	1.47
29	TZ122	0.65	0.46	0.29	0.48	0.49	0.50	0.81	6.51	0.43	0.89	1.81	1.40	1.49
30	TZ122	0.60	0.48	0.24	0.40	0.50	0.52	0.75	5.21	0.42	0.85	1.85	1.34	1.45
31	TZ50	0.72	0.43	0.47	0.97	0.51	0.51	0.73	6.63	0.39	0.84	1.86	1.40	1.39
32	TZ15	0.87	0.56	0.70	2.09	0.54	0.50	1.24	4.96	0.41	1.15	1.55	1.32	1.44
33	YM7	1.44	0.60	0.06	0.13	0.39	0.42	0.66	3.55	0.30	0.80	1.90	1.24	1.18
34	YM32	1.50	0.58	0.07	0.13	0.39	0.42	0.64	7.83	0.31	0.79	1.91	1.44	1.20
35	YM321	1.42	0.54	0.06	0.15	0.39	0.37	0.70	6.72	0.31	0.82	1.88	1.40	1.20
36	YM321	1.52	0.59	0.06	0.13	0.39	0.43	0.62	5.08	0.32	0.77	1.93	1.33	1.21
37	YM33	1.47	0.59	0.07	0.13	0.40	0.42	0.60	7.54	0.30	0.76	1.94	1.43	1.17
38	YM34	1.41	0.56	0.06	0.13	0.40	0.41	0.75	8.02	0.27	0.85	1.85	1.45	1.10
39	YM35	1.45	0.57	0.08	0.15	0.41	0.44	0.62	7.29	0.27	0.77	1.93	1.43	1.10
40	YM35	1.45	0.59	0.07	0.14	0.40	0.43	0.60	5.67	0.36	0.76	1.94	1.36	1.31
41	YM41	1.53	0.57	0.09	0.17	0.42	0.46	0.81	8.75	0.31	0.88	1.82	1.47	1.19
42	YM2	0.77	0.35	0.35	0.54	0.49	0.53	0.69	3.71	0.44	0.82	1.88	1.25	1.50
43	TD2	1.00	0.40	0.26	0.51	0.41	0.36	0.61	4.87	0.28	0.77	1.93	1.32	1.11

Abbreviations: – = no detection; $20S = 20S/(S + R)$ ratio for C_{29}-ααα steranes; $ββ = αββ/(ααα + αββ)$ ratio for C_{29} steranes; MDBT = methyldibenzothiophene; MDI = methyldiamantane index (4-MD/[4- + 1- + 3-MD]); MDR = methyldibenzothiophene ratio (4- MDBT/1- MDBT); MPI-1 = methylphenanthrene index 1 ($1.5 \times$ [2-MP + 3-MP]/[P + 1-MP + 9-MP]); nd = not determined; Pr/Ph = pristine/phytane; R_c1-1 = calculated equivalent vitrinite reflectance ($0.6 \times$ MPI-1 + 0.4) (Radke and Welte, 1983); R_c1-2 = $-0.6 \times$ MPI-1 + 2.30 (Radke and Welte, 1983); R_c2 = $0.263 \times$ Ln (MDR) + 0.9034 (Dzou et al., 1995); R_c3 = $2.4389 \times$ MDI + 0.4363 (Chen et al., 1996); TD = Tadong; T/P = tricyclic/pentacyclic terpane; T/(T + H) = C_{23} tricyclic terpane/(C_{23} tricyclic terpane + C_{30} 17α,21β(H)-hopane); Tm = 18α(H)-22,29,30-Trisnorhopane; Ts = 17α(H)-22,29,30-Trisnorhopane; TZ = Tazhong; YM = Yingmai; ZG = Zhonggu.
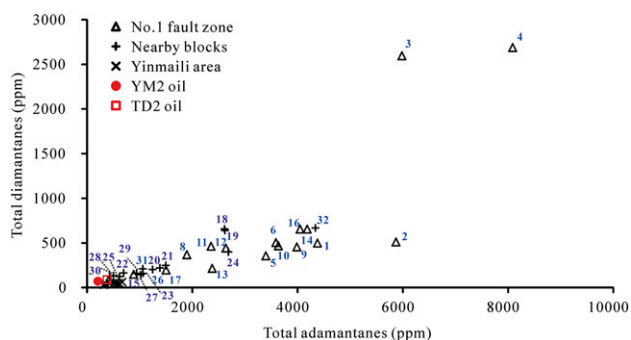
Figure 5. Cross plot of concentrations of adamantanes and diamantanes for Tarim oils. The label numbers refer to the sample numbers listed in Table 1. TD2 = Tadong 2; YM2 = Yingmai 2.

The oils from the Tazhong uplift in this study can be broadly divided into two groups based on the distribution of C_{27}, C_{28}, and C_{29} regular steranes and the abundance of gammacerane (Figures 3, 4, Table 1, Figures S2, S3, supplementary material available as AAPG Datashare 90 at www.aapg.org/datashare). Group I oils are mainly associated with the Tazhong No. 1 fault zone in the northern part of the Tazhong uplift and the TZ111, TZ122, TZ12, TZ50, TZ15, TZ451, and TZ47 wells of the nearby blocks. Their C_{27}, C_{28}, and C_{29} regular sterane distribution has a V shape, and they contain minor gammacerane (Figures 3, 4, Figures S2, S3, supplementary material available as AAPG Datashare 90 at www.aapg.org/datashare). These are typical characteristics of source rocks collected from the Middle–Upper Ordovician strata (Zhang et al., 2000), suggesting that group I oils are predominantly derived from the Middle–Upper Ordovician source rocks. The group II oils, including those from the TZ452-47 block close to the Tazhong No. 1 fault zone, are characterized by a linear or anti-L shape of the C_{27}, C_{28}, and C_{29} regular sterane distribution and a relatively high abundance of gammacerane, typical for oils that originated from the Cambrian–Lower Ordovician (Zhang et al., 2000; Li et al., 2010). This suggests that group II oils were produced by Cambrian–Lower Ordovician sources. No biomarkers have been detected for oils from the TZ721 (samples 18 and 19), TZ722 (sample 20), TZ83 (sample 21), and ZG1 (sample 24) wells in this work. The origin of these oils could not be established based on their biomarkers. In comparison to oils of groups I and II, oils within the Yingmaili section of the Luntai uplift have a higher Ph/Pr ratio, lower C_{23} tricyclic/(C_{23} tricyclic + C_{30}

hopane) ratio, and lower ratio of tricyclic to pentacyclic terpanes (Table 3), which is characteristic for oils from Luntai that are thought to be derived from Jurassic or possibly Triassic lacustrine source rocks within the Kuche depression (Hanson et al., 2000). Therefore, the oils of the Luntai area in this study are classified as group III oils for source identification of diamondoids.

The concentrations of individual diamondoid compounds within the oil samples analyzed during this study are given in Table S1 (supplementary material available as AAPG Datashare 90 at www.aapg.org/datashare). Figure 5 shows that the analyzed oils are characterized by different concentrations of adamantanes and diamantanes. For example, oils from the Tazhong No. 1 fault zone contain relatively high concentrations of adamantanes and diamantanes (887.1–8088 ppm total adamantanes; 147.1–2687 ppm total diamantanes), whereas oils from the Yingmaili area of the Luntai uplift contain lower concentrations of diamondoids (311.7–669.5 ppm total adamantanes; 29.5–60.0 ppm total diamantanes). All other oils have concentrations between these two. In general, condensates have higher concentrations of diamondoids than the normal and heavy oils in the Tazhong uplift; the lacustrine oils from the Yingmaili area have relatively lower concentrations of diamondoids than the normal marine oils from the Tazhong area. Therefore, the abundance of diamondoids within oils is controlled by both thermal maturity and the source of the oil, with the latter being especially important for oils within the oil window.

It is known that the quantity of the matrix (equal to the oil or soluble extraction of the source rock) changes during the thermal evolution of an oil or a source rock. Consequently, the diamondoid concentration of the oil or source rock is associated not only to the absolute quantity of diamondoid hydrocarbons but also to the quantity of the matrix. However, the concentration ratios of diamondoids do not correlate with the quantity of the matrix (Fang et al., 2013). The comparison of the concentration ratios of diamondoid pairs can thus eliminate the effect of matrix changes during the identification of oil sources. Variations in ratios for a few diamondoid pairs (adamantane [A]/methyladamantanes [MAs] versus MAs/dimethyladamantanes [DMAs], A/diamantane [D] versus MAs/MDs, and A/D versus 1-MA/4-MD) within oils in the Tarim Basin are shown in Figure 6
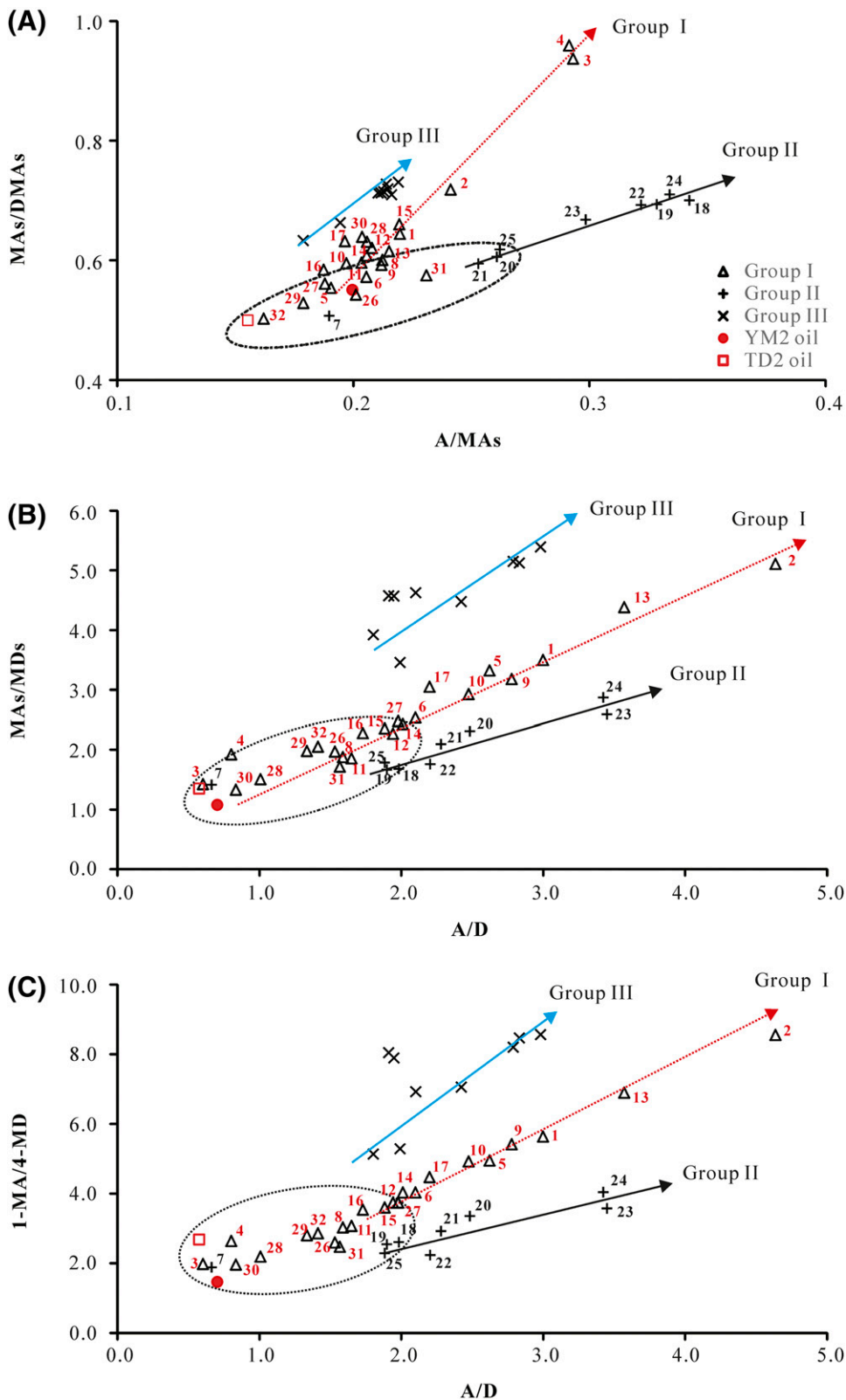
Figure 6. Cross plots of concentration ratios of adamantanes (As) and diamantanes (Ds) for Tarim oils: (A) A/methyl-adamantanes (MAs) versus MAs/dimethyladamantanes (DMAs), (B) A/D versus MAs/methyl-diamantanes (MDs), and (C) A/D versus 1-MA/4-MD. The label numbers refer to the sample numbers listed in Table 1. TD2 = Tadong 2; YM2 = Yingmai 2.
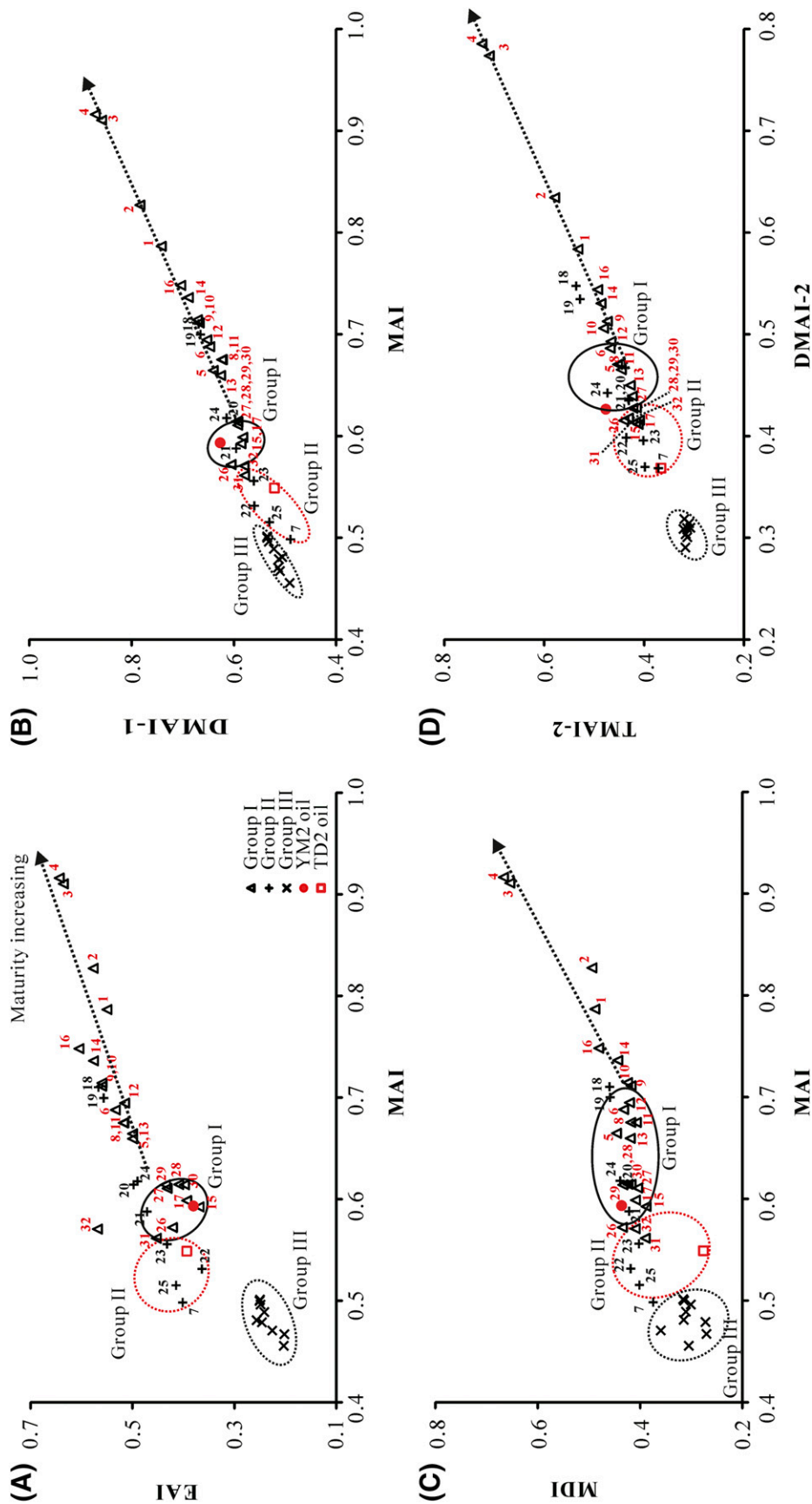
Figure 7. Cross plots of isomerization ratios of diamondoids for Tarim Basin oils. (A) Methyladamantane (MA) index (MAI) (1-MA/[1-MA + 2-MA]) versus ethyladamantane (EA) index (EAI) (1-EA/[1-EA + 2-EA]), (B) MAI versus dimethyladamantane (DMA) index 1 (DMAI-1) (1,3-DMA/[1,2-DMA + 1,3-DMA]), (C) MAI versus methyldiamantane (MD) index (MDI) (4-MD/[1-MD + 3-MD + 4-MD]), and (D) dimethyladamantane index 2 (DMAI-2) (1,3-DMA/[1,3-DMA + 1,4-DMA]) versus trimethyladamantane (TMA) index 2 (TMAI-2) (1,3,5-TMA/[1,3,5-TMA + 1,3,6-TMA]). The label numbers refer to the sample numbers listed in Table 1. TD2 = Tadong 2; YM2 = Yingmai 2.

(corresponding data are shown in Table S2, supplementary material available as AAPG Datashare 90 at www.aapg.org/datashare). Notably, except the normal and heavy oils with relatively lower concentration ratios, different group oils can be easily identified in Figure 6, plotting along different trend lines. Both normal and heavy oils within groups I and II plot in a relatively concentrated area with low concentration ratios of diamondoids in Figure 6 (dashed circle), with YM2 (group I) and TD2 (group II) oils also plotting in this area. Lacustrine oils from the Yingmaili area of the Luntai uplift define a third group of oils that show a different distribution in Figure 6 compared with the group I and II oils. It is notable that oils from the TZ721 (samples 18 and 19), TZ722 (sample 20), TZ83 (sample 21), and ZG17 (sample 24) wells, which cannot be grouped based on the biomarker compositions, as we stated earlier, can be classified according to the cross plots in Figure 6; they plot along the trend line of group II. Oils from TZ451 (sample 23) and TZ47 (sample 25) also plot on the line of group II, which is inconsistent with the biomarker characteristics indicating that those two oils are associated with group I (Table 1). This might be because of the mixing of oils from the Cambrian–Lower Ordovician strata with Middle–Upper Ordovician source rocks. Taking into consideration that biomarkers are minor compounds of the oils and that they are prone to be contaminated by oils with relatively higher biomarker contents from other source rocks, we suggest that those two oils are dominated by oils generated from the Cambrian–Lower Ordovician strata and were contaminated by Middle–Upper Ordovician oils.

Several diamondoid isomerization ratios, including the ethyladamantane (EA) index (EAI [1-EA/{1-EA + 2-EA}]) and the dimethyldiamantane indices (DMDI-1 [4,9-DMD/{4,9-DMD + 3,4-DMD}] and DMDI-2 [4,9-DMD/{4,9-DMD + 4,8-DMD}]), are also indicative of the sourcing of oils, and thermal maturity and biodegradation have no effect on DMDI-1 and DMDI-2 values (Schulz et al., 2001). The data presented in Fang et al. (2013) show that diamondoid isomerization ratios (e.g., methyladamantane index [MAI; 1-MA/{1-MA + 2-MA}], dimethyladamantane index 1 [DMAI-1; 1,3-DMA/{1,2-DMA + 1,3-DMA}], dimethyladamantane index 2 [DMAI-2; 1,3-DMA/{1,3-DMA + 1,4-DMA}], trimethyladamantane index 1 [TMAI-1; 1,3,5-TMA/{1,3,5-TMA + 1,3,4-TMA}], and trimethyladamantane index 2 [TMAI-2; 1,3,5-TMA/{1,3,5-TMA + 1,3,6-TMA}]) in oils are also unaffected by thermal maturity levels with EasyR_o (Sweeney and Burnham, 1990) values less than 2.0%, suggesting that oils from the same source with relatively low maturities should have a small range of isomerization ratios. However, significant differences in isomerization ratio values might be caused by changes in source rock facies. Figure 7 (corresponding data are shown in Table S2, supplementary material available as AAPG Datashare 90 at www.aapg.org/datashare) clearly separates the normal and heavy oils within the three oil groups defined above, demonstrating that oils with relatively low maturity have diamondoid isomerization ratios that are source dependent and therefore can be used for oil–oil correlation of normal and even heavy oils. Thus, a wide range of oils, including heavy oils, normal oils, and condensates, can be grouped based on the combination of the diamondoid concentration indices in Figure 6 and the isomerization ratios in Figure 7. And the classification result based on Figures 6 and 7 further supports the fact that group I oils were predominantly derived from the Middle–Upper Ordovician source rocks, whereas group II oils were produced by Cambrian–Lower Ordovician sources because the group I oils were grouped with the end-member oil (YM2) derived from the Middle–Upper Ordovician rocks, whereas group II oils were grouped with the end-member oil (TD2) produced from the Cambrian–Lower Ordovician rocks (Figure 7).

Maturity Determination

Biomarker and aromatic hydrocarbon ratios related to the oil maturity have been measured in the present study, such as $20S/(S + R)$ and $\alpha\beta\beta/(\alpha\alpha\alpha + \alpha\beta\beta)$ for the C_{29} steranes, $Ts/(Ts + Tm)$, MPI-1, and MDR. The C_{29} $20S/(S + R)$ sterane ratios of group I and group II oils range from 0.46 to 0.58 (Table 3), suggesting that these oils are mature ($R_o > 0.7\%$) because this ratio reaches its equilibrium point of 0.52–0.55 (Seifert and Moldowan, 1986; Peters et al., 2005). The C_{29} $\alpha\beta\beta/(\alpha\alpha\alpha + \alpha\beta\beta)$ sterane ratio ranges from 0.40 to 0.61 but does not reach its equilibrium (0.67–0.71; Seifert and Moldowan, 1986; Peters et al., 2005). Thus, most of the biomarker maturity indicators of the steranes and hopanes may have lost their effectiveness.

However, the values of the C_{29} $20S/(S + R)$ sterane and the C_{29} $\alpha\beta\beta/(\alpha\alpha\alpha + \alpha\beta\beta)$ sterane ratios of the group III oils are in the ranges of 0.39–0.49 and 0.36–0.53, respectively, suggesting that the oils of this group have a relatively lower maturity than those of groups I and II oils. The $Ts/(Tm + Ts)$ ratio is applicable over a wide range, from immature to mature to postmature; however, it strongly depends on the source (Peters et al., 2005). Table 3 shows that most of the oils in groups I and II range from 0.41 to 0.57, except for some exceptionally high or low values, whereas the oils in group III all approach 0.6, and it is hard to distinguish their maturity. Table 3 shows that MPI-1 $[1.5 \times (2\text{-MP} + 3\text{-MP})/(P + 1\text{-MP} + 9\text{-MP})]$ proposed by Radke and Welte (1983) ranges from 0.45 to 1.28. Because the MPI-1 shows a good positive linear correlation with the R_o in the oil window (0.65%–1.35% R_o) but a negative trend at higher maturity (1.35%–2.0% R_o) (Radke and Welte, 1983), two sequences of calculated equivalent R_o values (R_c1-1 and R_c1-2) have been determined based on MPI-1. The R_c1-1 values are mainly in the range of 0.70%–0.90% for all the three groups of oils, whereas the R_c1-2 values of most oils are close to 2.0% (Table 3). The maturity parameter of MDR (4-MDBT/1-MDBT) was proposed by Radke et al. (1986) and is considered to be particularly useful for the measurement of high-level maturities (Dzou et al., 1995). Another equivalent R_o (R_c2) can be derived based on the formula R_c2 (%) = 0.26338 × ln (MDR) + 0.9034 (Dzou et al., 1995). The R_c2 values suggest that these oils are highly mature (1.18%–1.64% for group I and group II oils and 1.24%–1.47% for group III oils; Table 3).

We also calculated the equivalent R_o (R_c3) based on the diamondoid index MDI (Table 3), which was proposed by Chen et al. (1996). The R_c3 values of group I and II oils range from 1.35% to 1.64%, except for the two TZ261 oils (2.03% and 2.06%), whereas those of group III oils are in the range of 1.10%–1.50%, similar to the result for R_c2. The difference of R_c1, R_c2, and R_c3 might be caused by several factors. The inconsistencies might be related to problems with respect to the calculation of the indices because the equations we used are the empirical relationships based on data for individual basins or regions, which might change in different areas. For example, the type of organic matter and migration could affect the methylphenanthrene ratios (Peters et al., 2005), which in turn affects the empirical relationship. However, multiple hydrocarbon charges to petroleum accumulations could also cause the discrepancy because different compound classes may be generated at different maturation stages. For example, diamondoid hydrocarbons are probably generated at later maturation stages than most aromatic hydrocarbons (Zhang et al., 2005). Additionally, oil mixtures from more than one source or different maturity stages of a source rock can lead to inconsistencies (Zhang et al., 2005). We suggest that the sterane parameters are more effective in investigating relatively low mature oils, whereas the methyldibenzothiophene and diamondoid indices are probably more reliable for the evaluation of the maturity of highly mature oils such as that of group I and II.

It is widely accepted that diamondoid indices (e.g., MAI and MDI) can be used to determine the thermal maturity of highly mature crude oils (R_o > 1.1%; Chen et al., 1996) and that higher diamondoid concentrations are indicative of higher thermal maturities (Chen et al., 1996; Dahl et al., 1999). Chen et al. (1996) first proposed the relationship between MDI and the R_o and inferred that the maturity of the crude oils in the Tarim Basin is generally greater than 1.1% R_o, whereas gases and condensates from the Yinggehai and Qiongdongnan basins in China have maturities equivalent to 1.6%–2.0% R_o. The MDI index has also been used as a maturity parameter for highly mature and overmature carbonate source rocks in the Shangangning Basin in China; it has been suggested that the MDI index cannot be used to measure the maturities of source rocks with a maturity greater than 2.0% R_o (Li et al., 2000). However, Figures 5–7 reveal that diamondoid abundances and ratios within oils are also related to hydrocarbon sources. Wei et al. (2006) reported that diamondoid abundances in various source rocks (including types I and II of organic matter of terrestrial or marine input) are generally an order of magnitude higher than the abundances of diamondoids within coals under the same thermal maturity conditions. The present study indicates that group III lacustrine oils contain lower concentrations of diamondoids than group I and II marine oils (Figure 5), with distinct diamondoid ratio trends (Figures 6, 7). This finding suggests that the evaluation of oil maturity using diamondoid abundance and ratios should only be performed on oils with similar sources.
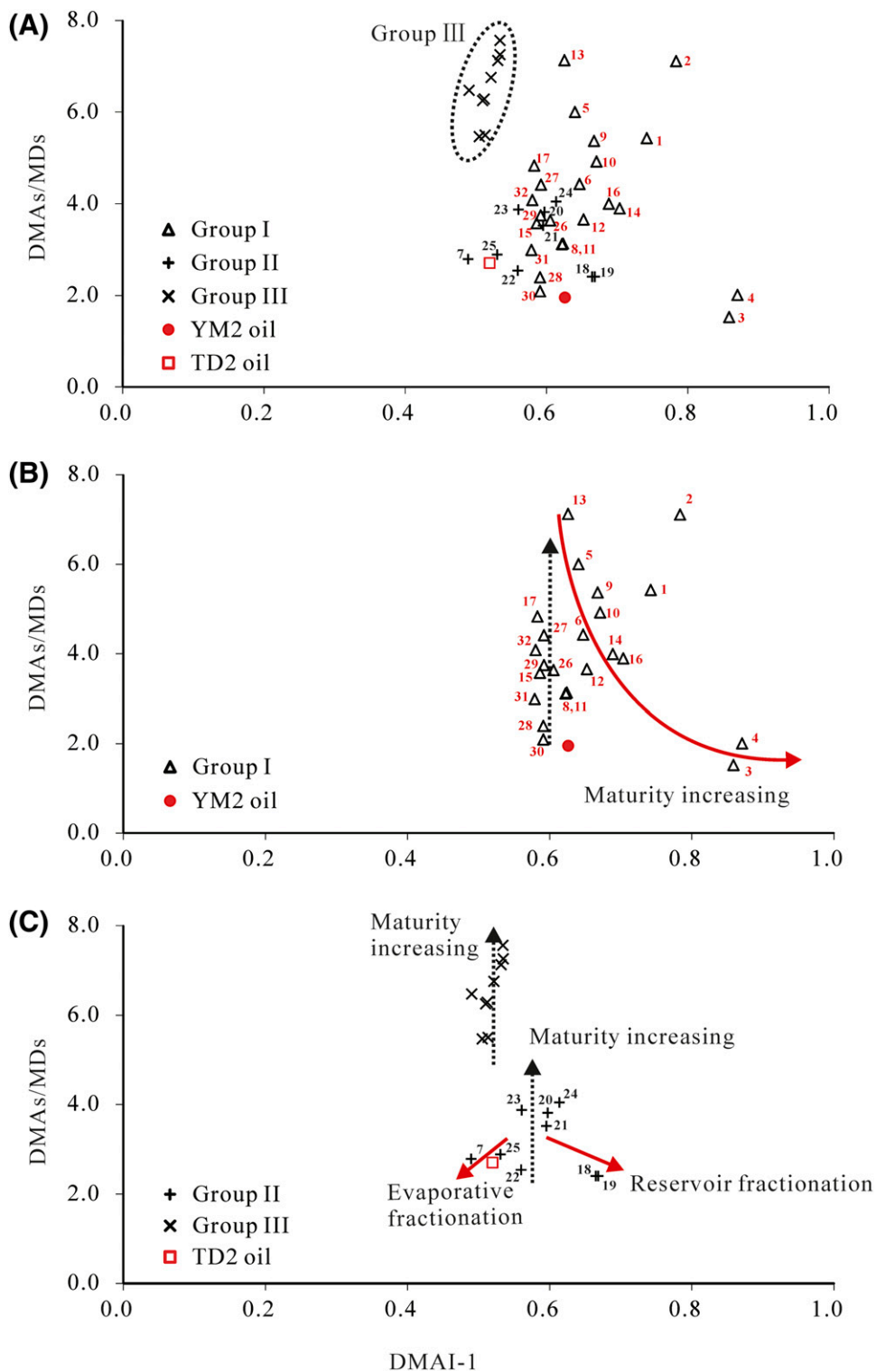
Figure 8. Cross plots of dimethyladamantane index 1 (DMAI-1; 1,3-DMA/[1,2-DMA + 1,3-DMA]) versus dimethyladamantanes (DMAs)/methyldiamantanes (MDs) for Tarim Basin oils. (A) Distribution of group I, group II, and group III oils in the cross plot. (B) Distribution of group I oils in the cross plot. (C) Distribution of group II and group III oils in the cross plot. TD2 = Tadong 2; YM2 = Yingmai 2.

Different diamondoid indices are suitable for different maturity ranges (Fang et al., 2013) because diamondoid concentration ratios show a positive correlation with thermal maturity during the early stages of oil cracking (corresponding to EasyR$_o$ 1.0%–2.0%) but a negative correlation with EasyR$_o$ values of greater than 2.0%. Diamondoid isomerization ratios show a positive correlation with thermal maturity during the later stages of oil cracking (corresponding to EasyR$_o$ > 2.0%). This result of Fang et al. (2013) shows that diamondoid concentration ratios can be used to assess the maturity of oils with EasyR$_o$ 1.0%–2.0% and diamondoid isomerization ratios can be used for the assessment of highly mature condensates (EasyR$_o$ > 2.0%). Oils within the oil window (EasyR$_o$ 0.5%–1.0%) have diamondoid concentrations and distributions that are dependent on the source instead of maturity, suggesting that diamondoid analysis cannot be used to determine the maturity of oils within the oil window; however, traditional biomarker methods can be used at this stage of thermal maturity.

The concentrations of diamondoids vary significantly within the oils analyzed during this study, indicating that oils within the Tarim Basin have a wide range of thermal maturity; this is especially true for oils from the Tazhong No. 1 fault zone (Figure 5). Figure 7 shows that all group III oils have similar diamondoid isomerization ratios, and the majority of group II oils also have similar values to each other, suggesting their thermal maturity is less than 2.0% (EasyR$_o$) because the diamondoid isomerization ratios are almost unaffected by thermal maturity levels when EasyR$_o$ < 2.0% (Fang et al., 2013). Diamondoid concentration ratios can also be used to assess thermal maturity levels, and an increasing oil maturity trend is clearly evident for group II and III oils in Figure 6. Furthermore, Figures 6 and 7 also show that the group I oils have highly variable thermal maturities. Oils from the TZ261 (samples 3 and 4) and TZ826 (sample 16) wells have low concentration ratios (Figure 6B, C) but high concentrations of diamondoids within these oils (Figure 5), demonstrating that these oils have undergone at least some cracking and suggesting that they have entered a higher thermal maturity stage (EasyR$_o$ > 2.0%). Figure 7 also shows that oils from the TZ26 (samples 1 and 2), TZ261 (samples 3 and 4), TZ826 (sample 16), and TZ821 (sample 14)

wells have maturities that can be assessed using diamondoid isomerization ratios, although the thermal maturity of the majority of the group I oils can be evaluated more accurately using diamondoid concentration ratios (Figure 6B, C).

Fang et al. (2013) suggested that more refined maturity assessments can be obtained by plotting diamondoid concentrations against diamondoid isomerization ratios. This is shown in Figure 8, in which the constant DMAI-1 values of group II and III oils are indicative of the early stages of oil cracking (Figure 8C), whereas group I oils have a wide range of thermal maturities and have diamondoid parameters that define a thermal evolution trend similar to that found by Fang et al. (2013) (Figure 8B). In addition, Figures 6 and 7 indicate that the thermal maturity of Ordovician oils associated with the Tazhong No. 1 fault zone is independent of burial depth (Table 1) and increases from west to east (Figures 1B, 6, 7). One possible explanation for this trend is that highly mature condensates located in the eastern part of the Tazhong No. 1 fault zone represent a late stage of hydrocarbon charging, with these condensates migrating from a deeper, older, and more mature source.

Factors other than thermal maturation, such as biodegradation, evaporation, and other reservoir fractionations such as gas washing (Zhang et al. 2011), can also affect the concentration and composition of diamondoids within oils, leading to changes in the distributions shown in Figures 6–8. This is exemplified by waxy TZ721 oils (samples 18 and 19) that have higher A/MAs ratios (Figure 6A). Jia et al. (2013) used carbon and hydrogen isotope analysis of individual n-alkanes to suggest that these waxy oils are a mix of highly mature oils generated from Middle–Upper Ordovician and Cambrian–Lower Ordovician sources. However, Figure 6 clearly shows that these waxy oils are closely related to the group II oils, but the TZ721 oils have higher MAI, DMAI-1, and DMAI-2 ratios than group II oils (Figures 7, 8C). These variations could be explained by reservoir fractionation. In addition, TD2 and TZ62 (sample 7) oils have relatively low DMAI-1 and DMAs/MDs ratios (Figure 8C) that may relate to evaporative fractionation because this process causes the preferential loss of diamondoid compounds with relatively low boiling points and therefore decreases the DMAs/MDs and DMAI-1 ratios of residual oils (Li et al., 2014).

Extent of Oil Cracking

The term "oil cracking" broadly refers to the thermal breakdown of heavy hydrocarbons to lighter hydrocarbons during the maturation of crude oil (Dahl et al., 1999). This process is an important evolutionary step for the formation of condensate oils and gases in the deeper sections of basins. The diamondoid method of Dahl et al. (1999) has been widely used to estimate the extent of oil cracking. However, experiments performed by Fang et al. (2012) suggest that there are three main stages of oil cracking: condensate generation (1.0%–1.5% $EasyR_o$), wet gas generation (1.5%–2.1% $EasyR_o$), and dry gas generation (2.1%–4.5% $EasyR_o$). The first stage of oil cracking is dominated by the thermal breakdown of C_{13+} hydrocarbons to form C_6–C_{12} hydrocarbons, with a lack of oil mass loss showing that the concentrations of 4- + 3-methyldiamantane in oils are insensitive to this early stage of cracking. However, the wet gas stage of oil cracking (>1.5% $EasyR_o$) is associated with the generation of gaseous hydrocarbons, a process that is associated with oil mass loss. This suggests that diamondoid concentrations can be used to estimate the degree of oil cracking once the wet gas stage has been entered. Given this, we use the term oil cracking to describe the thermal breakdown of liquid to gaseous hydrocarbons.

The extent of oil cracking (EOC; i.e., the percentage of liquid hydrocarbons converted to gas and pyrobitumen) can be calculated using the following formula (Dahl et al., 1999):

$$EOC(\%) = [1 - (C_0/Cc)] \times 100 \qquad (1)$$

where C_0 is the concentration of 4- + 3-methyldiamantane in uncracked oils (i.e., the methyldiamantane baseline) and Cc is the concentration of 4- + 3-methyldiamantane in cracked oils derived from the same source. Oils within the same basin from different sources probably have their own diamondoid baselines, indicating that the use of this method to determine EOC values is reliant on accurately determining these baseline values (i.e., C_0). However, it is still unclear how to determine the methyldiamantane baseline of an oil source. Assigning too low a baseline value would mean that a large number of normal oils would be incorrectly considered to be cracked oils, and the EOC values of lightly cracked oils would possibly be overestimated.

Dahl et al. (1999) suggested that the diamondoid baseline can be inferred by analyzing a group of uncracked, nonbiodegraded, and nonfractionated oils derived from a single source. However, the fact that the oils that meet these conditions cover a wide range of thermal maturity means that the 4- + 3-methyldiamantane concentrations of these oils also vary. In general, the values of relatively low-maturity, nonbiodegraded, and nonfractionated oils are used as baselines for groups of oils and are therefore used to estimate EOC values for other oils. Previous research has shown that substantial amounts of 4- + 3-methyldiamantane can be generated both during diagenesis and during oil formation (Fang et al., 2012, 2013). This demonstrates that the identification of the onset of oil cracking, and the related concentration of 4- + 3-methyldiamantanes within oils at this stage of thermal maturity, is critical
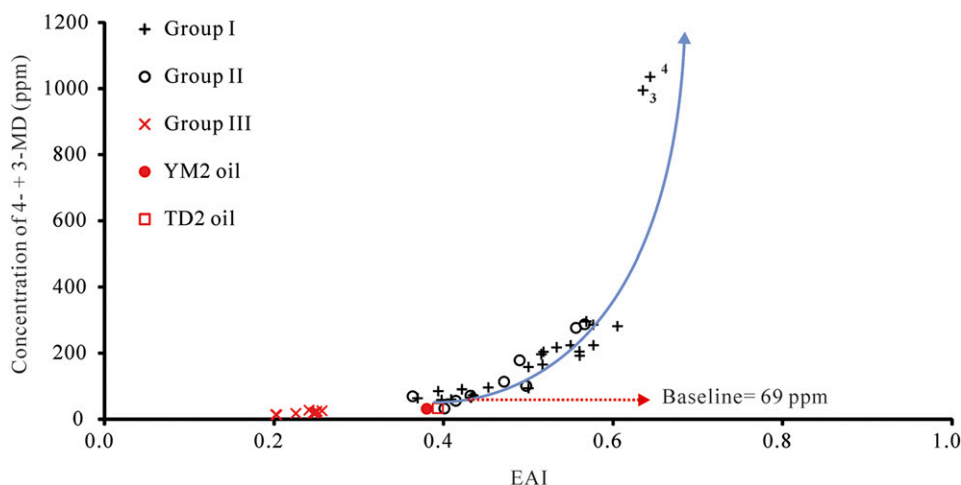

Figure 9. Cross plot of ethyladamantane (EA) index (EAI; 1-EA/[1-EA + 2-EA]) versus concentration of 4- + 3-methyldiamantanes (MDs) for Tarim Basin oils. TD2 = Tadong 2; YM2 = Yingmai 2.

when using the method of Dahl et al. (1999) to assess the extent of oil cracking in reservoirs.

Based on the definition of oil cracking in the present study, the concentration of 4- + 3-methyldiamantanes in oils at a thermal maturity of approximately 1.5% EasyR$_o$ should be a good estimate of the methyldiamantane baseline for a given oil source. Fang et al. (2013) reported that oil cracking is associated with an increase in EAI values and that this increase starts at a thermal maturity of 1.5% EasyR$_o$. This indicates that a positive correlation between EAI values and the concentration of 4- + 3-methyldiamantane in oil is indicative of the start of the wet gas stage of oil cracking, and as such, plotting these values together can yield the methyldiamantane baseline value. Figure 9 shows that the group I and II oils of this study have similar trends, with 4- + 3-methyldiamantane concentrations showing a positive correlation with EAI values of greater than 0.43. This shows that the average 4- + 3-methyldiamantane concentrations of oils with EAI values of 0.41–0.43 can be considered as the methyldiamantane baseline value for group I and II oils. This calculation yields a value of approximately 69 ppm, which is used to assess EOC values for marine oils within the Tarim Basin. In comparison, group III oils contain low concentrations of 4- + 3-methyldiamantane (Figure 9). Other diamondoid parameters also indicate that these oils have not undergone cracking, and therefore, the methyldiamantane baseline of these oils cannot be determined. The EOC data of cracked oils are provided in Table S2 (supplementary material available as AAPG Datashare 90 at www.aapg.org/datashare).

The overestimation of EOC values using the diamondoid method was identified by correlating mass balance–based cracking estimates with values determined using diamondoid concentrations and equation 1, and these overestimates are attributed to the evaporative loss of lighter hydrocarbons from oils (Dahl et al., 1999). Here we suggest that selecting low baseline values can also lead to the overestimation of EOC values. In addition, the further generation of 4- + 3-methyldiamantanes at EasyR$_o$ values of greater than 2.0% (Fang et al., 2013) can lead to the overestimation of EOC values. This is exemplified by two condensates from the TZ261 well (samples 3 and 4). The EAI values of these oils (0.64) and the relationship between EAI values and the thermal maturity of marine oils

within the Tarim Basin established by Fang et al. (2013) suggest that these two condensates underwent thermal maturation at EasyR$_o$ values of greater than 2.0%. Therefore, some of the diamondoids within these two oils were generated during late-stage charging of the reservoir, a process that was accompanied by oil cracking. This signifies that the EOC values calculated using equation 1 (93.3% for sample 3 oil and 93.1% for sample 4 oil) are probably overestimates of the extent of cracking of these oils.

Origin of the Oil Accumulation in the Tazhong Uplift

The Tazhong uplift comprises multiple types of oils ranging from condensate to heavy oil and covering a wide range of maturity, indicating complex processes related to hydrocarbon generation, migration, and accumulation. The Cambrian–Lower Ordovician source rocks reached the oil window in the Late Ordovician, whereas the Middle–Upper Ordovician source rocks were still immature (Tian et al., 2008; Jia et al., 2013). The Middle–Upper Ordovician strata were marginally mature from the Permian to Cretaceous (Tian et al., 2008). The oil and gas accumulations in the Tazhong uplift were thus initially charged by hydrocarbons generated from the Cambrian–Lower Ordovician source rocks during the Late Ordovician (Tian et al., 2008). The late Caledonian orogeny led to the destruction of these early reservoirs, before this area was recharged by hydrocarbons from the Middle–Upper Ordovician source rocks (Tian et al., 2008; Pan and Liu, 2009). Therefore, the group II oils distributed in the blocks west of the No. 1 fault (Figure 1B) probably represent the residue of these early-formed oils derived from the Cambrian–Lower Ordovician source rocks. They have a relatively lower thermal maturity and no relationship with the No. 1 fault, which had already formed by the Late Ordovician. The Cambrian–Lower Ordovician source rocks entered into a highly mature to overmature stage at the end of the Cretaceous and generated light oils and gases. At the same time, the Middle–Upper Ordovician source rocks began to mature; the normal oils in group I represent the oils generated in this period. The deeply buried Middle–Upper Ordovician source rocks evolved

into a highly mature stage in the Tertiary and produced light oils and gases (Jia et al., 2013). Faults and unconformities in the Tazhong area were important factors during the migration and accumulation of the hydrocarbons, as shown by the Tazhong No. 1 fault. The Tazhong No. 1 fault, which formed during the middle–late Caledonian orogeny, cut the Cambrian, Ordovician, and Sinian strata. It connected the deep source rocks of the Tazhong uplift with the adjacent depressions and allowed the migration of hydrocarbons generated from different source rocks with various maturities to the Tazhong uplift.

The oil reservoirs distributed along the Tazhong No. 1 fault zone were recharged by the oils generated in the later stages through the fault zone. Pang et al. (2013) proposed that the intersection point of the northwest-trending faults and the northeast-trending faults in the Tazhong uplift is the injection point of the hydrocarbons and that the maturity of the oils decreases with the increase of the distance from the injection point. The hydrocarbon supply was insufficient during the later period of oil generation. The hydrocarbons with higher maturity generated in the later stage primarily charged the reservoirs in the areas proximal to the injection points. Consequently, the oils of this study, which are proximal to the No. 1 fault, will have higher maturities than those relatively far from the fault. This is consistent with the lower maturity of group I oils in the eastern blocks (TZ111, sample 26; TZ12, samples 27 and 28; TZ122, samples 29 and 30; TZ50, sample 31; and TZ15, sample 32) compared with oils distributed along the Tazhong No. 1 fault (Figure 8B). This also explains the presence of heavy oils in group I (TZ111, sample 26; TZ12, samples 27 and 28; TZ122, sample 29; TZ50, sample 31; and TZ15, sample 32), which might contribute to less recharge of oils with higher maturity.

It is notable that group I contains heavy oils. As stated above, the generation by the marginally mature Middle–Upper Odovician source rocks from the Permian to Cretaceous and the lower charge of hydrocarbons with higher maturity during the later period might be the reasons for the occurrence of heavy oils. In addition, heavy oils collected from the Silurian reservoirs (TZ111, sample 26; TZ12, sample 27, TZ122, sample 29; TZ50, sample 31; and TZ15, sample 32) might be attributed to the alteration of bitumen in the Silurian sandstone by the recharged

oils (Xiao et al., 2000; Tian et al., 2008). The Cambrian–Lower Ordovician source rocks entered the peak oil generation stage during the middle Silurian to Early Devonian (Xiao et al., 2000). The oils generated during this stage migrated from faults and unconformity surfaces into the Silurian sandstone and accumulated. However, the oil reservoirs in the Silurian strata were destroyed because of the escape of light hydrocarbons or biodegradation of hydrocarbons associated with the early Hercynian orogeny in the Late Devonian (Figure 2) (Li et al., 2010), leading to solid bitumen sandstone reservoirs (Xiao et al., 2000; Tian et al., 2008). The oils generated from the Middle–Upper Ordovician source rocks during the later period then recharged those bituminous sandstone reservoirs, and the bitumen was altered to a type of heavy oil (Xiao et al., 2000). Additionally, thermal alteration of crude oils might also be one of the reasons for the formation of heavy oils, which is typical for the TD2 heavy oil in group II (Zhang and Huang, 2005; Tang and Wang, 2007).

CONCLUSIONS

Approaches based on the concentration and distribution of diamondoids in crude oils enabled an investigation of possible sources and the thermal maturity of oils within the Tazhong and Luntai uplifts.

1. The oils analyzed during this study can be divided into three groups based on the diamondoid indices and biomarker characteristics: group I oils are mainly derived from Middle–Upper Ordovician units instead of Cambrian–Lower Ordovician source rocks; group II oils predominantly originate from Cambrian–Lower Ordovician units; and group III oils were generated from Jurassic or possibly Triassic lacustrine sources, which contain lower concentrations of diamondoids and have different biomarker and diamondoid parameters compared with group I and II oils.
2. The oils in group I distributed along the Tazhong No. 1 fault have higher maturities (>2.0% EasyR$_o$), whereas heavy oils in the nearby blocks have relatively lower maturities (<2.0% EasyR$_o$). The oils both in group II and III have a constant diamondoid isomerization ratio, suggesting that their thermal maturities are less than 2.0% EasyR$_o$. In combination

with the oil accumulation history of the Tazhong uplift, it is suggested that the group I oils were mainly charged or recharged by late-generated hydrocarbons derived from Middle–Upper Ordovician sources, whereas group II oils were dominated by early-charged hydrocarbons sourced from Cambrian–Lower Ordovician units.

3. We also proposed an approach to obtain baseline 4- + 3-methyldiamantane concentrations to estimate the extent of oil cracking. This approach shows that the Tarim Basin marine oils have a baseline value of approximately 69 ppm.

REFERENCES CITED

Chen, J. H., J. M. Fu, G. Y. Sheng, D. H. Liu, and J. Zhang, 1996, Diamondoid hydrocarbon ratios: Novel maturity indices for highly mature crude oils: Organic Geochemistry, v. 25, p. 179–190, doi:10.1016/S0146-6380 (96)00125-8.

Dahl, J. E., J. M. Moldowan, K. E. Peters, G. E. Claypool, M. A. Rooney, G. E. Michael, M. R. Mello, and M. L. Kohnen, 1999, Diamondoid hydrocarbons as indicators of natural oil cracking: Nature, v. 399, p. 54–57, doi:10.1038/19953.

Dzou, L. I. P., R. A. Noble, and J. T. Senftle, 1995, Maturation effects on absolute biomarker concentration in a suite of coals and associated vitrinite concentrates: Organic Geochemistry, v. 23, p. 681–697, doi:10.1016/0146-6380(95)00035-D.

Fang, C. C., Y. Q. Xiong, Y. Li, Y. Chen, J. Z. Liu, H. Z. Zhang, A. A. Taofik, and P. A. Peng, 2013, The origin and evolution of adamantanes and diamantanes in petroleum: Geochimica et Cosmochimica Acta, v. 120, p. 109–120, doi:10.1016/j.gca.2013.06.027.

Fang, C. C., Y. Q. Xiong, Q. Y. Liang, and Y. Li, 2012, Variation in abundance and distribution of diamondoids during oil cracking: Organic Geochemistry, v. 47, p. 1–8, doi:10.1016/j.orggeochem.2012.03.003.

Hanson, A. D., S. C. Zhang, J. M. Moldowan, D. G. Liang, and B. M. Zhang, 2000, Molecular organic geochemistry of the Tarim Basin, northwest China: AAPG Bulletin, v. 84, no. 8, p. 1109–1128, doi:10.1306/A9673C52-1738-11D7-8645000102C1865D.

Huang, D. F., B. W. Liu, T. D. Wang, Y. C. Xu, S. J. Chen, and M. J. Zhao, 1999, Genetic type and maturity of Lower Paleozoic marine hydrocarbon gases in the eastern Tarim Basin: Chemical Geology, v. 162, p. 65–77, doi:10.1016/S0009-2541(99)00053-4.

Jia, W. L., P. A. Peng, C. L. Yu, and Z. Y. Xiao, 2010, Molecular and isotopic compositions of bitumens in Silurian tar sands from the Tarim Basin, NW China: Characterizing biodegradation and hydrocarbon charging in an old composite basin: Marine and Petroleum Geology, v. 27, p. 13–25, doi:10.1016/j.marpetgeo.2009.09.003.

Jia, W. L., Q. L. Wang, P. A. Peng, Z. Y. Xiao, and B. H. Li, 2013, Isotopic compositions and biomarkers in crude oils from the Tarim Basin: Oil maturity and oil mixing: Organic Geochemistry, v. 57, p. 95–106, doi:10.1016/j .orggeochem.2013.01.002.

Li, D. S., D. G. Liang, C. Z. Jian, G. Wang, Q. Z. Wu, and D. F. He, 1996, Hydrocarbon accumulations in the Tarim Basin, China: AAPG Bulletin, v. 80, no. 10, p. 1587–1603.

Li, J., P. Philp, and M. Cui, 2000, Methyl diamantane index (MDI) as a maturity parameter for lower Plaeozoic carbonate rocks at high maturity and overmaturity: Organic Geochemistry, v. 31, p. 267–272, doi:10.1016/S0146-6380(00)00016-4.

Li, S. M., X. Q. Pang, Z. J. Jin, H. J. Yang, Z. Y. Xiao, Q. Y. Gu, and B. S. Zhang, 2010, Petroleum source in the Tazhong uplift, Tarim Basin: New insights from geochemical and fluid inclusion data: Organic Geochemistry, v. 41, p. 531–553, doi:10.1016/j.orggeochem.2010.02.018.

Li, Y., Y. Q. Xiong, Y. Chen, and Y. J. Tang, 2014, The effect of evaporation on the concentration and distribution of diamondoids in oils: Organic Geochemistry, v. 69, p. 88–97, doi:10.1016/j.orggeochem.2014.02.007.

Liang, D. G., Q. Y. Gu, and X. J. Pi, 1998, Distribution law of the condensate gas reservoirs in Tabei uplift (in Chinese): Natural Gas Industry, v. 18, p. 5–9.

Liang, D. G., S. C. Zhang, B. M. Zhang, and F. Y. Wang, 2000, Understanding on marine oil generation in China based on Tarim Basin (in Chinese): Earth Science Frontiers, v. 7, p. 534–547.

Liang, Q. Y., Y. Q. Xiong, C. C. Fang, and Y. Li, 2012, Quantitative analysis of diamondoids in crude oils using gas chromatography – triple quadrupole mass spectrometry: Organic Geochemistry, v. 43, p. 83–91, doi:10.1016/j.orggeochem.2011.10.008.

Liu, R., J. Y. Shi, and X. M. Zheng, 1994, A discussion on the geochemical characteristics and unconventional evaluation method of high altered carbonate rocks (in Chinese): Natural Gas Industry, v. 14, p. 62–66.

Lu, X. X., Z. J. Jin, L. F. Liu, S. L. Xu, X. Y. Zhou, X. J. Pi, and H. J. Yang, 2004, Oil and gas accumulations in the Ordovician carbonates in the Tazhong Uplift of Tarim Basin, west China: Journal of Petroleum Science & Engineering, v. 41, no. 1–3, p. 109–121, doi:10.1016/S0920-4105(03) 00147-5.

Pan, C. C., and D. Y. Liu, 2009, Molecular correlation of the free oil, adsorbed oil and inclusion oil of reservoir rocks in the Tazhong uplift of the Tarim Basin, China: Organic Geochemistry, v. 40, p. 387–399, doi:10.1016/j .orggeochem.2008.11.005.

Pang, H., J. Q. Chen, X. Q. Pang, K. Y. Liu, L. F. Liu, C. F. Xiang, and S. M. Li, 2013, Analysis of secondary migration of hydrocarbons in the Ordovician carbonate reservoirs in the Tazhong uplift, Tarim Basin, China: AAPG Bulletin, v. 97, no. 10, p. 1765–1783, doi:10.1306/04231312099.

Peters, K. E., C. C. Walters, and J. M. Moldowan, 2005, The biomarker guide: Biomarkers and isotopes in petroleum exploration and Earth history: Cambridge, United Kingdom, Cambridge University Press, v. 2, 700 p.

Radke, M., and D. H. Welte, 1983, The methylphenanthrene index (MPI): A maturity parameter based on aromatic hydrocarbons, *in* M. Bjorøy, P. Albrecht, C. Cornford, K. de Groot, G. Eglinton, E. Galimov, D. Leythaeuser, R. Pelet, J. RullkÖtter, and G. Speers, eds., Advances in organic geochemistry 1981: New York, John Wiley and Sons, p. 504–512.

Radke, M., D. H. Welte, and H. Willsch, 1986, Maturity parameters based on aromatic hydrocarbons: Influence of the organic matter type: Organic Geochemistry, v. 10, p. 51–63, doi:10.1016/0146-6380(86)90008-2.

Schulz, L. K., A. Wilhelms, E. Rein, and A. S. Steen, 2001, Application of diamondoids to distinguish source rock facies: Organic Geochemistry, v. 32, p. 365–375, doi: 10.1016/S0146-6380(01)00003-1.

Seifert, W. K., and J. M. Moldowan, 1986, Use of biological markers in petroleum exploration, *in* R. B. Johns, ed., Methods in geochemistry and geophysics 24, Amsterdam, Elsevier, p. 261–290.

Su, J., S. C. Zhang, H. P. Huang, Y. Wang, H. T. Wang, K. He, X. M. Wang, B. Zhang, and H. J. Wang, 2016, New insights into the formation mechanism of high hydrogen sulfide-bearing gas condensates: Case study of Lower Ordovician dolomite reservoirs in the Tazhong uplift, Tarim Basin: AAPG Bulletin, v. 100, no. 6, p. 893–916, doi:10.1306/02101615081.

Sun, Y. G., S. P. Xu, H. Lu, and P. X. Chai, 2003, Source facies of the Paleozoic petroleum systems in the Tabei uplift, Tarim Basin, NW China: Implications from aryl isoprenoids in crude oils: Organic Geochemistry, v. 34, p. 629–634, doi:10.1016/S0146-6380(03)00063-9.

Sweeney, J. J., and A. K. Burnham, 1990, Evaluation of a simple model of vitrinite reflectance based on chemical-kinetics: AAPG Bulletin, v. 74, no. 10, p. 1559–1570.

Tang, Y. J., and T. G. Wang, 2007, Molecular fossils and oil-source rock correlations of Cambrian heavy oil in Tadong 2 well in Tarim Basin (in Chinese): Journal of China University of Petroleum, v. 11, p. 18–22.

Tian, H., X. M. Xiao, R. W. T. Wilkins, H. J. Gan, Z. Y. Xiao, D. H. Liu, and L. G. Guo, 2008, Formation and evolution of Silurian paleo-oil pools in the Tarim Basin, NW China: Organic Geochemistry, v. 39, p. 1281–1293, doi: 10.1016/j.orggeochem.2008.05.011.

Wang, F. Y., S. C. Zhang, B. M. Zhang, Z. Y. Xiao, and C. W. Liu, 2003, Maturity and its history of Cambrian marine source rocks in the Tarim Basin (in Chinese): Geochimica, v. 32, p. 461–468.

Wei, Z., J. M. Moldowan, D. M. Jarvie, and R. Hill, 2006, The fate of diamondoids in coals and sedimentary rocks: Geology, v. 12, p. 1013–1016, doi:10.1130/G22840A.1.

Wei, Z., J. M. Moldowan, K. E. Peters, Y. Wang, and W. Xiang, 2007, The abundance and distribution of diamondoids in biodegraded oils from the San Joaquin Valley: Implications for biodegradation of diamondoids in petroleum reservoirs: Organic Geochemistry, v. 38, p. 1910–1926, doi:10.1016/j.orggeochem.2007.07.009.

Wingert, W. S., 1992, GC-MS analysis of diamondoid hydrocarbons in Smackover petroleum: Fuel, v. 71, p. 37–43, doi:10.1016/0016-2361(92)90190-Y.

Xiao, X. M., Z. G. Song, D. H. Liu, Z. F. Liu, and J. M. Fu, 2000, The Tazhong hybrid petroleum system, Tarim Basin, China: Marine and Petroleum Geology, v. 17, p. 1–12, doi:10.1016/S0264-8172(99)00050-1.

Xiao, Z., Y. Lu, Y. Wu, F. Y. Zhao, L. Qian, and Y. A. Jin, 2005, A preliminary study on natural gas genesis and pool-forming period in the Silurian reservoir of well Mandong 1, east Tarim Basin (in Chinese): Chinese Journal of Geology, v. 34, p. 155–160.

Yu, S., C. C. Pan, J. J. Wang, X. D. Jin, L. L. Jiang, D. Y. Liu, X. X. Lü et al., 2012, Correlation of crude oils and oil components from reservoirs and source rocks using carbon isotopic compositions of individual n-alkanes in the Tazhong and Tabei uplift of the Tarim Basin, China: Organic Geochemistry, v. 52, p. 67–80, doi:10.1016/j.orggeochem.2012.09.002.

Zhang, S. C., A. D. Hanson, J. M. Moldowan, S. A. Graham, D. G. Liang, E. Chang, and F. Fago, 2000, Paleozoic oil-source rock correlations in the Tarim basin, NW China: Organic Geochemistry, v. 31, p. 273–286, doi:10.1016/S0146-6380(00)00003-6.

Zhang, S. C., and H. P. Huang, 2005, Geochemistry of Palaeozoic marine petroleum from the Tarim Basin, NW China: Part 1. Oil family classification: Organic Geochemistry, v. 36, p. 1204–1214, doi:10.1016/j.orggeochem.2005.01.013.

Zhang, S. C., H. P. Huang, Z. Y. Xiao, and D. G. Liang, 2005, Geochemistry of Palaeozoic marine petroleum from the Tarim Basin, NW China. Part 2: Maturity assessment: Organic Geochemistry, v. 36, p. 1215–1225, doi:10.1016/j.orggeochem.2005.01.014.

Zhang, S. C., J. Su, X. M. Wang, G. Y. Zhu, H. J. Yang, K. Y. Liu, and Z. X. Li, 2011, Geochemistry of Palaeozoic marine petroleum from the Tarim Basin, NW China: Part 3. Thermal cracking of liquid hydrocarbons and gas washing as the major mechanisms for deep gas condensate accumulations: Organic Geochemistry, v. 42, p. 1394–1410, doi:10.1016/j.orggeochem.2011.08.013.